

# Lockdown: a non-pharmaceutical policy to prevent the spread of COVID-19. Mathematical modeling and computation

Subhendu PAUL and Emmanuel LORIN

the date of receipt and acceptance should be inserted later

**Abstract** In this paper, we derive and analyze an extended SIRS-model which includes lockdown policies at the early stages of the pandemic. The latter play a salient role for flattening the curve of infectious diseases such as COVID-19, and is introduced as a model compartment. An error function is reported, which serves as a bridge between the outcomes of the model and available databases; we estimate the values of the model parameters by minimizing the error function. The intervention function, obtained from the equivalent system of the proposed model, and effective reproduction function are also derived to understand the underline scenario of the coronavirus outbreak. We then estimate the epidemiological variables such as susceptible, recovered, lockdown etc. for Canada and three of its provinces, Ontario, Québec and British Columbia, significantly affected by the coronavirus. Some improvements, such as spatial dependence or “at risk” vs “healthy” population, will finally be proposed in order to increase the accuracy of the modeling.

Keywords: Dynamical system, epidemiology, COVID-19, optimization, data.

## 1 Introduction

The outbreak of coronavirus [22,36,31,39] (COVID-19), an infectious disease caused by a newly discovered virus, SARS-CoV-2 (commonly known as coronavirus), is a serious pandemic currently affecting the world. The virus is mainly transmitted through droplets generated when an infected person coughs, sneezes, or exhales. A person can be infected by breathing if he/she is within close proximity of someone who has COVID-19, or by touching a contaminated surface and then touching his/her eyes, nose or mouth. Coronavirus employs densely glycosylated spike protein to penetrate human host cells. The virus applies a nested set of mRNAs to replicate, and the replication of the viral RNA occurs when RNA polymerase binds and re-attaches to multiple locations [28,15].

COVID-19, a new disease, cases officially emerged as early as December 2019 when a strange medical condition was first reported at Wuhan in China. This virus has an overall mortality rate of 10% [30], which makes it more severe than the common flu. People who have other pre-existing illnesses such as respiratory disease, diabetes are succumbing more to COVID-19. People with only mild symptoms recover within 3 to 7 days, while those with pneumonia or severe diseases take weeks to recover. The recovery percentage of patients, for example, in China was 51% [30]. At that time, the recovery percentage of COVID-19 was expected to reach 90% [30]. The infection was reported to have spread to many cities across China over January 2020, with thousands in China becoming infected by the disease, while also spreading rapidly and globally, affecting countries including Thailand, Japan, Korea, Vietnam, Singapore, United States,

---

S. Paul  
School of Mathematics and Statistics, Carleton University, Ottawa, Canada, K1S 5B6. E-mail: subhendu.paul@carleton.ca  
E. Lorin  
School of Mathematics and Statistics, Carleton University, Ottawa, Canada, K1S 5B6. Centre de Recherches Mathématiques, Université de Montréal, Montréal, Canada, H3T 1J4. E-mail: elorin@math.carleton.ca

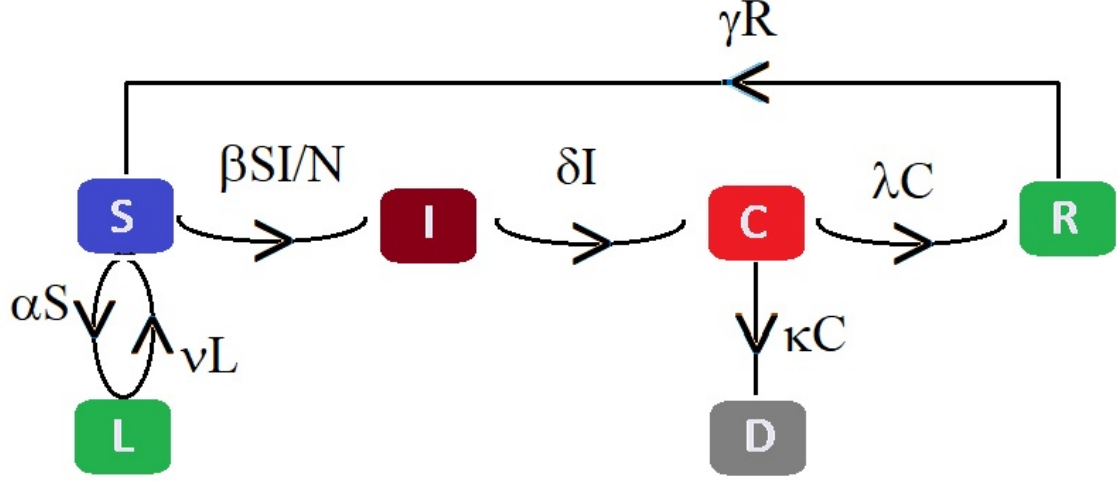


Fig. 1 Schematic diagram of the compartmental epidemic model, presented in Equation (1).

Canada etc. [37]. The World Health Organization (WHO) declared the outbreak a pandemic on March 11, 2020 and, as of July 15, 2020, a total of 13,150,645 confirmed cases of COVID-19 worldwide have been reported by WHO with 574,464 related deaths. In this paper, we will specifically study the case of Canada, and some of its provinces during the so called *first wave*, from January 25, 2020 to July 10, 2020.

**Pandemic in Canada:** According to the government report [3], the novel coronavirus arrived on the Canadian coast at least as early as January 25, 2020 with a traveler from Wuhan, China. Since February 9, 2020, the Canadian Government has imposed COVID-19 testing requirements for travelers returning from affected areas to 10 airports across 6 provinces. On February 20, the Canadian Government confirmed first corona-positive case of a traveler arriving Canada from outside mainland China. The Canadian Government confirmed the first COVID-19 death on March 9. On March 13, the Canadian Government advised Canadians to avoid non-essential travels outside of Canada until further notice. On March 16, the Canadian Government advised travelers entering Canada to isolate themselves for 14 days. Preventative measures aimed at minimizing transmission were increasingly imposed by the Canadian Government from March 18, 2020, foreigners from all countries except the United States having prohibited entry to Canada, and 14 days of self-quarantining imposed for returning citizens; the Canada-United States border was closed for all non-essential travel and redirected arrivals of international passenger flights to four airports in Calgary, Vancouver, Toronto and Montréal. The Canadian Government has imposed the screening restriction; that is all passengers traveling to Canada will be screened prior to boarding on March 30. On April 2, the Canadian Government launched the ‘Canada COVID-19 app’ on iOS and Android to provide Canadians with the latest information on COVID-19 and a possibility of online self-assessment.

Preventing the spread of COVID-19 caused by the new SARS-CoV2 was a big challenge at the early stage of the pandemic, as there was no vaccines or other appropriate drugs. In that situation, lockdown (home quarantine, social distancing and using personal protective equipment) was played a crucial role in controlling the pandemic.

Since the outbreak of the COVID-19 pandemic, a numerous number of mathematical model-based simulations have been published. The latter are mainly using Susceptible-Infected-Recovered (SIR) or modified SIR type models [38,35,4,9,24,32,17], allowing to deduce important epidemiological parameters, such as ‘reproduction number’ as well as various intervention scenarios [6,7,11,14,16,21,25,29,13,18,27,22]. In addition, infectious disease models can be employed to estimate salient epidemiological parameters via data simulation methods [7,12,23,33,8]. In the SIRS model, the population is divided into the susceptible  $S$ , infected  $I$  and recovered  $R$  groups, and their relative growths and competition are represented as a set of coupled ordinary differential equations. The model cannot capture the large-scale effects of more granular interactions, such as lockdown. In the context, we need a sophisticated disease model including the lockdown phenomenon to study the early stage of the current pandemic more precisely. But naturally, the derived model could be applied to study the similar situation.

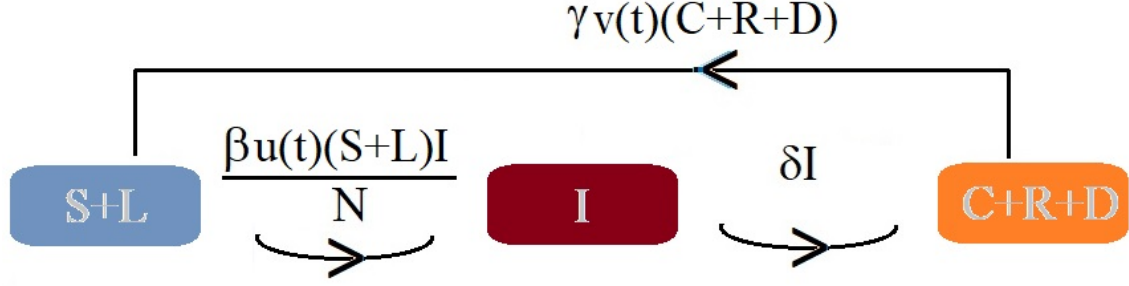


**Fig. 2** Schematic diagram of the equivalent system, presented in Equation (5).

In the article, we introduce an original extended SIRS model, summarized in Figure 1, including the non-pharmaceutical policy lockdown and a total of six compartments. Those partitions are Lockdown, Susceptible, Infected, Corona positive cases, Recovered and Deaths (L-SICRD). Mathematically the model can be presented as a set of coupled ordinary differential equations involving several parameters. We consider all the possible transmissions among the parts, and the model parameters are linked to these diffusions. In the current scenario, the model parameters are treated as constants (time-independent) but in principle, one can consider the model parameters as a function of time which involves significant additional computational cost. The article shows the exponential growth phase at the early stage of the COVID-19 epidemic in Canada as well as in some of its provinces where the coronavirus has been considerably affected.

This paper is organized as follows. The detailed description of the model as well as the simulation procedure to estimate the parameters of the model are presented in Section 2. In Section 3, we present some analytical results such as local and global stability for the disease-free equilibrium as well as endemic equilibrium. In Section 4, we report the calculated results with a brief discussion. Section 5 is devoted to some possible improvements of the model. This will include spatial dependence, the introduction of population subgroups, as well as the study of lockdown scenarios thanks to optimization techniques. Some final remarks are exposed in Section 6.

## 2 Epidemiological modelling

In this section, we construct an infectious disease model L-SICRD for COVID-19 which includes a lockdown variable. The model is constructed as a set of coupled ordinary differential equations involving several variables and parameters. We also derive the effective reproduction function from an equivalent system.

### 2.1 The Mathematical Model

Modeling the spread of epidemics is an essential tool for projecting its outcome. By estimating important epidemiological parameters using the available database, we can make forecasts of different intervention scenarios. In the context of compartment based models, where the population of a region is distributed into several sub-populations, such as susceptible, infected, recovered, deceased etc., is a simple but useful tool to demonstrate the panorama of an epidemics.

In this article, we introduce an infectious disease model, extending the standard SIRS model, including the phenomenon lockdown, a non-pharmaceutical way to prevent the spread of the epidemics. The model system is illustrated in Figure 1 with several compartments and various model parameters. The following are the underlying principles of the present model.

- The total population is constant (neglecting the migrations, births and unrelated deaths) and initially every individual is susceptible to contract the disease.
- The disease is spread through the direct (face-to-face meeting) or indirect (through air current, common used or delivery items like door handles, grocery products) contact of susceptible individuals with the infective individuals.

- The quarantined area or the compartment for corona cases contains only members of the infected population who are tested corona-positive.
- The virus always kills to some percent of the people it infects; the survivors percent represents the recovered group.
- Individuals who recover do not have immunity, and there is a possibility of transmission from recovered to susceptible individuals.
- There is a non-pharmaceutical policy (stay at home), commonly known as *lockdown*, to stop the spread of the disease.
- We ignore the phenomenon of recovered individuals from the asymptomatic group. If someone died in COVID-19, it was recorded.

Based on the above principles, we consider six compartments:

- Susceptible ( $S$ ): the group of individuals who can be infected.
- Infected ( $I$ ): the group of people who are spreading the contagious disease including asymptomatic individuals.
- Corona cases ( $C$ ): the group of individuals who are tested corona-positive.
- Recovered ( $R$ ): the group of individuals who eventually survive.
- Deaths ( $D$ ): the group of individuals who deceased.
- Lockdown (insusceptible) ( $L$ ): a combination of mass policy as well as individual choice of self-isolation; the group of persons who are keeping themselves safe.

The time-dependent model is the following set of coupled ordinary differential equations:

$$\begin{cases} \frac{dS}{dt} = -\beta \frac{SI}{N} - \alpha S + \gamma R + \nu L, \\ \frac{dI}{dt} = \beta \frac{SI}{N} - \delta I, \\ \frac{dC}{dt} = \delta I - \lambda C - \kappa C, \\ \frac{dR}{dt} = \lambda C - \gamma R, \\ \frac{dD}{dt} = \kappa C, \\ \frac{dL}{dt} = \alpha S - \nu L \end{cases} \quad (1)$$

where  $\alpha, \beta, \gamma, \delta, \lambda, \kappa$  and  $\nu$  are real positive parameters respectively modeling the rate of lockdown, the rate of infection, the rate of susceptibility, the rate of corona-positive cases, the rate of recovery, the rate of death and the rate of ignoring lockdown. The total number of infectious population at time  $t$  is  $I(t) + C(t)$ . We only have the publicly available data base of recovered and deaths who tested corona-positive. Therefore, in the model, recovered ( $R$ ) and deaths ( $D$ ) come from the compartment  $C$ . It follows from (1), that for any  $t$

$$S(t) + L(t) + I(t) + C(t) + R(t) + D(t) = N, \quad (2)$$

where  $N$  is the total (constant) population size. We can rewrite the system of coupled ordinary differential equations in a matrix form:

$$\frac{d\mathbf{Y}}{dt} = \mathbf{A}\mathbf{Y} + \mathbf{F} \quad (3)$$

$$\text{where } \mathbf{Y} = \begin{pmatrix} S \\ I \\ C \\ R \\ D \\ L \end{pmatrix}, \mathbf{A} = \begin{pmatrix} -\alpha & 0 & 0 & \gamma & 0 & \nu \\ 0 & -\delta & 0 & 0 & 0 & 0 \\ 0 & \delta & -(\lambda + \kappa) & 0 & 0 & 0 \\ 0 & 0 & \lambda & -\gamma & 0 & 0 \\ 0 & 0 & \kappa & 0 & 0 & 0 \\ \alpha & 0 & 0 & 0 & 0 & -\nu \end{pmatrix}, \text{ and } \mathbf{F} = SI \begin{pmatrix} -\frac{\beta}{N} \\ \frac{\beta}{N} \\ 0 \\ 0 \\ 0 \\ 0 \end{pmatrix}.$$

We will solve (3) using a standard 4th order Runge-Kutta method with particular sets of model parameters. To solve the initial value problem (3), in the interval  $[t_0, t_1]$ , we consider  $S(t_0), L(t_0), I(t_0), C(t_0),$

$R(t_0)$  and  $D(t_0)$  as follows:

$$\begin{cases} S(t_0) = N - L(t_0) - I(t_0) - C(t_0) - R(t_0) - D(t_0) \\ L(t_0) = q_1 \bar{C}(t_0) \\ I(t_0) = q_2 \bar{C}(t_0) \\ C(t_0) = \bar{C}(t_0) \\ R(t_0) = \bar{R}(t_0) \\ D(t_0) = \bar{D}(t_0), \end{cases} \quad (4)$$

where  $\bar{C}(t_0)$ ,  $\bar{R}(t_0)$  and  $\bar{D}(t_0)$  are the available data at time  $t_0$ , and  $q_1, q_2$  are the initial value adjusting parameters.

## 2.2 Effective reproduction function

In this subsection, we derive an equivalent system, composed of three chambers, of the proposed L-SICRD model. The diagram of the equivalent system is presented in Figure 2; the meaning of the variables  $S, L, I, C, R, D$  and the parameters  $\beta, \delta$  and  $\gamma$  are the same as above. However, there are two new time-dependent functions  $u(t)$  and  $v(t)$  in the equivalent model, where  $u(t)$  describes the modification of the transmission rate due to lockdown, and  $v(t)$  models the recovery rate. The purpose of the equivalent model is to calculate the effective reproduction number which is a function of time. The equivalent system can be represented by a set of coupled ordinary differential equations, for any  $t$ :

$$\begin{cases} \frac{d}{dt}(S + L) &= -\beta u(t) \frac{(S + L)I}{N} - \alpha S + \gamma R + \nu L, \\ \frac{dI}{dt} &= \beta u(t) \frac{(S + L)I}{N} - \delta I, \\ \frac{d}{dt}(C + R + D) &= \delta I - \gamma v(t)(C + R + D). \end{cases} \quad (5)$$

It follows from (1) and (5) that

$$v(t) := \frac{R(t)}{C(t) + R(t) + D(t)}, \quad (6)$$

and

$$u(t) := \frac{S(t)}{S(t) + L(t)}. \quad (7)$$

Now we define the basic ratio number  $\rho$  and effective reproduction function  $R_{\text{Eff}}(t)$  as follows:

$$\rho := \frac{\beta}{\delta}, \quad (8)$$

and

$$R_{\text{Eff}}(t) = \rho u(t). \quad (9)$$

From the second Equation of (5), we obtain the following conclusion:

- If  $R_{\text{Eff}}(t) < N/(S(t) + L(t))$ , each existing infection produces less than one new infection. In this case, the disease will decline and eventually die out.
- If  $R_{\text{Eff}}(t) = N/(S(t) + L(t))$ , each existing infection generates one new infection. The disease will persist and will be stable, but there will not be an outbreak or epidemic.
- If  $R_{\text{Eff}}(t) > N/(S(t) + L(t))$ , each existing infection originates more than one new infection. The disease will be transmitted between people, and there may be an outbreak or epidemic.

## 3 Mathematical analysis

In this section, we discuss the local and global stability of the disease-free equilibrium as well as endemic equilibrium. In addition, we derive basic reproduction number using a next generation matrix method [10].

### 3.1 Positivity and boundedness of the solutions

The L-SICRD model presented in Section 2.1 describes the evolution of human population, and therefore, all the quantities (lockdown, susceptible, infected, corona-positive cases, recovered and deaths) must be proven positive, for all time.

**Theorem 31** *The components of the solution to the L-SICRD model (1) are nonnegative for any given nonnegative initial condition.*

**Proof.** We can rewrite the system of coupled ordinary differential equations, defined in (1), in a matrix form:

$$\frac{d\mathbf{X}}{dt} = B\mathbf{X}, \quad (10)$$

where all  $t$ ,  $\mathbf{X}(t) = \begin{pmatrix} S(t) \\ I(t) \\ C(t) \\ R(t) \\ D(t) \\ L(t) \end{pmatrix}$  and  $B(t) = \begin{pmatrix} -\beta \frac{I(t)}{N} - \alpha & 0 & 0 & \gamma & 0 & \nu \\ 0 & \beta \frac{S(t)}{N} - \delta & 0 & 0 & 0 & 0 \\ 0 & \delta & -(\lambda + \kappa) & 0 & 0 & 0 \\ 0 & 0 & \lambda & -\gamma & 0 & 0 \\ 0 & 0 & \kappa & 0 & 0 & 0 \\ \alpha & 0 & 0 & 0 & 0 & -\nu \end{pmatrix}.$

Let us set

$$f(t) := \max \left\{ \beta \frac{I(t)}{N} + \alpha, \delta - \beta \frac{S(t)}{N}, \lambda + \kappa, \gamma, \nu \right\} + f_0, \quad (11)$$

where  $f_0$  is a positive constant. We can rewrite the matrix  $B(t)$  as  $B(t) = B_1(t) + B_2(t)$  where  $B_1(t) = -f(t)I_6$ , and

$$B_2(t) = \begin{pmatrix} f(t) - \beta \frac{I(t)}{N} - \alpha & 0 & 0 & \gamma & 0 & \nu \\ 0 & f(t) + \beta \frac{S(t)}{N} - \delta & 0 & 0 & 0 & 0 \\ 0 & \delta & f(t) - (\lambda + \kappa) & 0 & 0 & 0 \\ 0 & 0 & \lambda & f(t) - \gamma & 0 & 0 \\ 0 & 0 & \kappa & 0 & f(t) & 0 \\ \alpha & 0 & 0 & 0 & 0 & f(t) - \nu \end{pmatrix}.$$

It follows that all the elements of the matrix  $B_2$  are nonnegative, and hence, so are the entries of  $\exp \left( \int_0^t B_2(\xi) d\xi \right)$ . Moreover, we have

$$\exp \left( \int_0^t B_1(\xi) d\xi \right) = e^{-\int_0^t f(\xi) d\xi} I_6.$$

Then, as the matrix  $-f(t)I_6$  commutes with the matrix  $B_2$ , we have

$$\exp \left( \int_0^t B(\xi) d\xi \right) = \exp \left( \int_0^t B_1(\xi) d\xi \right) \exp \left( \int_0^t B_2(\xi) d\xi \right),$$

which implies that all the entries of the matrix  $\exp \left( \int_0^t B(\xi) d\xi \right)$  are nonnegative. Now from (11), we obtain that

$$\mathbf{X}(t) = \mathbf{X}(0) \exp \left( \int_0^t B(\xi) d\xi \right), \quad \text{for } t \geq 0. \quad (12)$$

such that  $X_i(0) \geq 0$  for all  $i \in \{1, \dots, 6\}$ . We conclude that  $X_i(t) \geq 0$  all  $i \in \{1, \dots, 6\}$  and all  $t \geq 0$ .  $\square$

The boundedness of the components of the solution  $L(t)$ ,  $S(t)$ ,  $I(t)$ ,  $C(t)$ ,  $R(t)$  and  $D(t)$  follows from the fact that  $L(t) + S(t) + I(t) + C(t) + R(t) + D(t) = N$  (the total population), in (2), and we obtain from Theorem 31 that  $L(t)$ ,  $S(t)$ ,  $I(t)$ ,  $C(t)$ ,  $R(t)$ ,  $D(t) \geq 0$ , for time  $t \geq 0$ . Therefore we have that each component of the solution is at most equal to  $N$  i.e., for all  $t \geq 0$ ,  $0 \leq S(t)$ ,  $L(t)$ ,  $I(t)$ ,  $C(t)$ ,  $R(t)$ ,  $D(t) \leq N$ , assuming that  $0 \leq S(0)$ ,  $L(0)$ ,  $I(0)$ ,  $C(0)$ ,  $R(0)$ ,  $D(0) \leq N$ . Thus the set of feasible solutions which is positively invariant set of the model, is given for  $t \geq 0$  by :

$$\Omega(t) := \{ (L, S, I, C, R, D) \in \mathbb{R}_+^6 / L(t) + S(t) + I(t) + C(t) + R(t) + D(t) = N \}. \quad (13)$$

### 3.2 Existence and uniqueness of solutions

The system of coupled differential equations, presented in (10), associated to the L-SICRD model can also be rewritten in the form

$$\frac{d\mathbf{X}}{dt} = \mathcal{F}(\mathbf{X}), \quad (14)$$

where

$$\begin{cases} \mathcal{F}_1(\mathbf{X}) = -\beta \frac{S(t)I(t)}{N} - \alpha S(t) + \gamma R(t) + \nu L(t), \\ \mathcal{F}_2(\mathbf{X}) = \beta \frac{S(t)I(t)}{N} - \delta I(t), \\ \mathcal{F}_3(\mathbf{X}) = \delta I(t) - (\lambda + \kappa)C(t), \\ \mathcal{F}_4(\mathbf{X}) = \lambda C(t) - \gamma R(t), \\ \mathcal{F}_5(\mathbf{X}) = \kappa C(t), \\ \mathcal{F}_6(\mathbf{X}) = \alpha S(t) - \nu L(t). \end{cases} \quad (15)$$

The function  $\mathcal{F}$  is continuous and bounded (since all solutions are bounded) in  $\mathbb{R}^6$ , as well as its partial derivatives are continuous and bounded in  $\mathbb{R}^6$ . Hence Peano's existence theorem in conjunction with Theorem 8.1 (on page 441) in [20] guarantees the existence of a unique global solution for the L-SICRD model.

### 3.3 Disease-free equilibrium

It is obvious that the system, defined in (1), always has the disease-free equilibrium  $\mathcal{E}_0 \in \Omega$  given by

$$\mathcal{E}_0 = (L_0, S_0, I_0, C_0, R_0, D_0) = \left( \frac{\alpha}{\alpha + \nu}(N - D_0), \frac{\nu}{\alpha + \nu}(N - D_0), 0, 0, 0, D_0 \right), \quad (16)$$

where  $D_0 (\geq 0)$  is the total number of death toll. The Jacobian of the disease-free equilibrium (DFE) state is given as:

$$J(L_0, S_0, I_0, C_0, R_0, D_0) = \begin{pmatrix} -\alpha & -\beta \frac{S_0}{N} & 0 & \gamma & 0 & \nu \\ 0 & \beta \frac{S_0}{N} - \delta & 0 & 0 & 0 & 0 \\ 0 & \delta & -(\lambda + \kappa) & 0 & 0 & 0 \\ 0 & 0 & \lambda & -\gamma & 0 & 0 \\ 0 & 0 & \kappa & 0 & 0 & 0 \\ \alpha & 0 & 0 & 0 & 0 & -\nu \end{pmatrix}. \quad (17)$$

### 3.4 Linearized system

The linearization of the system at the equilibrium point  $\mathcal{E}_0$  is

$$\begin{cases} \frac{dS}{dt} = -\alpha S - \beta \frac{S_0 I}{N} + \gamma R + \nu L, \\ \frac{dI}{dt} = \beta \frac{S_0 I}{N} - \delta I, \\ \frac{dC}{dt} = \delta I - \lambda C - \kappa C, \\ \frac{dR}{dt} = \lambda C - \gamma R, \\ \frac{dD}{dt} = \kappa C, \\ \frac{dL}{dt} = \alpha S - \nu L. \end{cases} \quad (18)$$

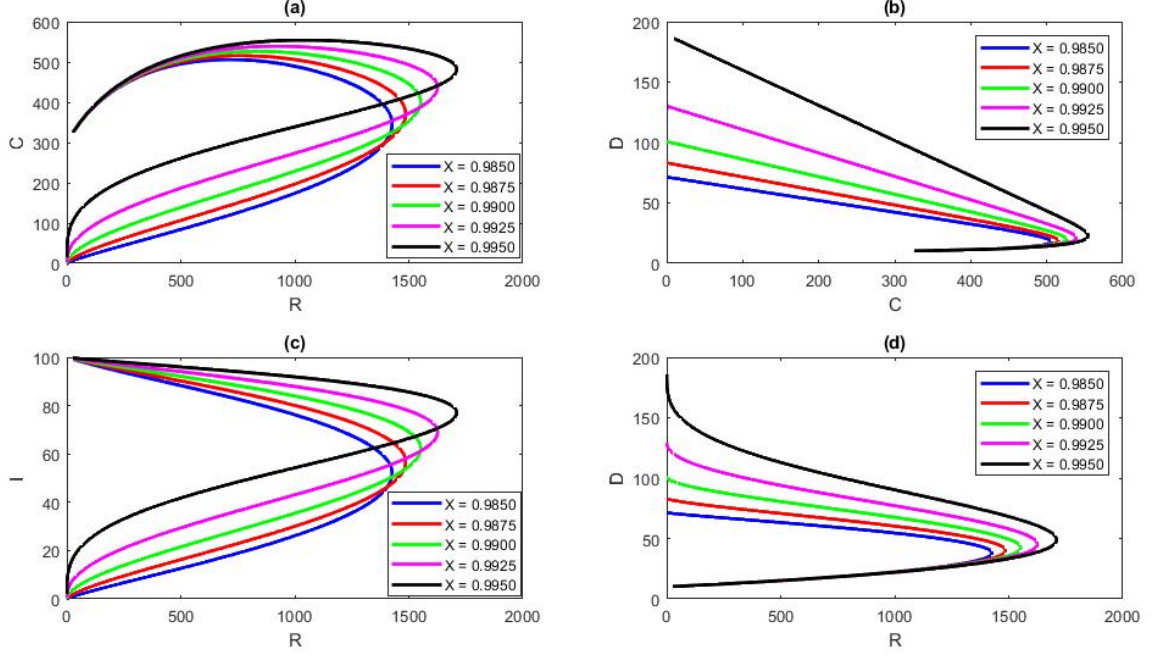


**Fig. 3** Solution of the linearized system (18) with Here  $X = \beta S_0/\delta N < 1$  : (a) Phase portrait of  $C(t)$  and  $R(t)$ . (b) Phase portrait of  $D(t)$  and  $C(t)$ . (c) Phase portrait of  $I(t)$  and  $R(t)$ . (d) Phase portrait of  $D(t)$  and  $R(t)$ .

Solving (18), leads to

$$\begin{cases} I(t) = I(0) \exp\left(\left(\beta \frac{S_0}{N} - \delta\right)t\right), \\ C(t) = C(0) \exp\left(-(\lambda + \kappa)t\right) + \frac{\delta I(0)}{\beta \frac{S_0}{N} - \delta + \lambda + \kappa} \left[ \exp\left(\beta \frac{S_0}{N} - \delta\right)t - \exp\left(-(\lambda + \kappa)t\right) \right], \\ D(t) = D(0) + \kappa \int_0^t C(\xi) d\xi, \\ R(t) = R(0) \exp(-\gamma t) + \lambda \exp(-\gamma t) \int_0^t C(\xi) d\xi. \end{cases} \quad (19)$$

To solve the linearized system (18) numerically, we consider the set of parameters values as  $\delta = 0.55$ ,  $\gamma = 0.0099$ ,  $\lambda = 0.09$ ,  $\kappa = 0.008$ , and four different values of  $\beta S_0/\delta N = X = 0.9850, 0.9875, 0.9900, 0.9925$ , and  $0.9950$  with initial values  $I(0) = 100, C(0) = 300, D(0) = 10, R(0) = 200$  and the total population  $N = 7500$ . As  $\beta S_0/\delta N < 1$ , and according to Theorems 32 and 33 the disease-free equilibrium  $\mathcal{E}_0 = (\sigma(N - D_0), (1 - \sigma)(N - D_0), 0, 0, 0, D_0)$  where  $0 \leq \sigma \leq 1$  of (1) is locally and globally stable, see Figures 3 and 4. The values of  $D_0$  depend on  $\beta S_0/\delta N$ ; for  $X = 0.9850, 0.9875, 0.9900, 0.9925$  and  $0.9950$ , we obtain  $D_0 = 71, 83, 100, 130$  and  $185$ , respectively. To verify the fact that the proposed model works locally, here we analyze the linear system.

### 3.5 Basic reproduction number

To calculate the basic reproduction number, we consider the linearized system (18), infection subsystem in the form

$$\frac{d}{dt} \begin{pmatrix} I \\ C \end{pmatrix} = (\mathcal{A} + \mathcal{B}) \begin{pmatrix} I \\ C \end{pmatrix}, \quad (20)$$

where  $\mathcal{A}$  and  $\mathcal{B}$ , are respectively the transmission matrix and transition matrix, defined as

$$\mathcal{A} = \begin{pmatrix} \beta S_0 & 0 \\ \delta & 0 \end{pmatrix}, \mathcal{B} = \begin{pmatrix} -\delta & 0 \\ 0 & -(\lambda + \kappa) \end{pmatrix}.$$



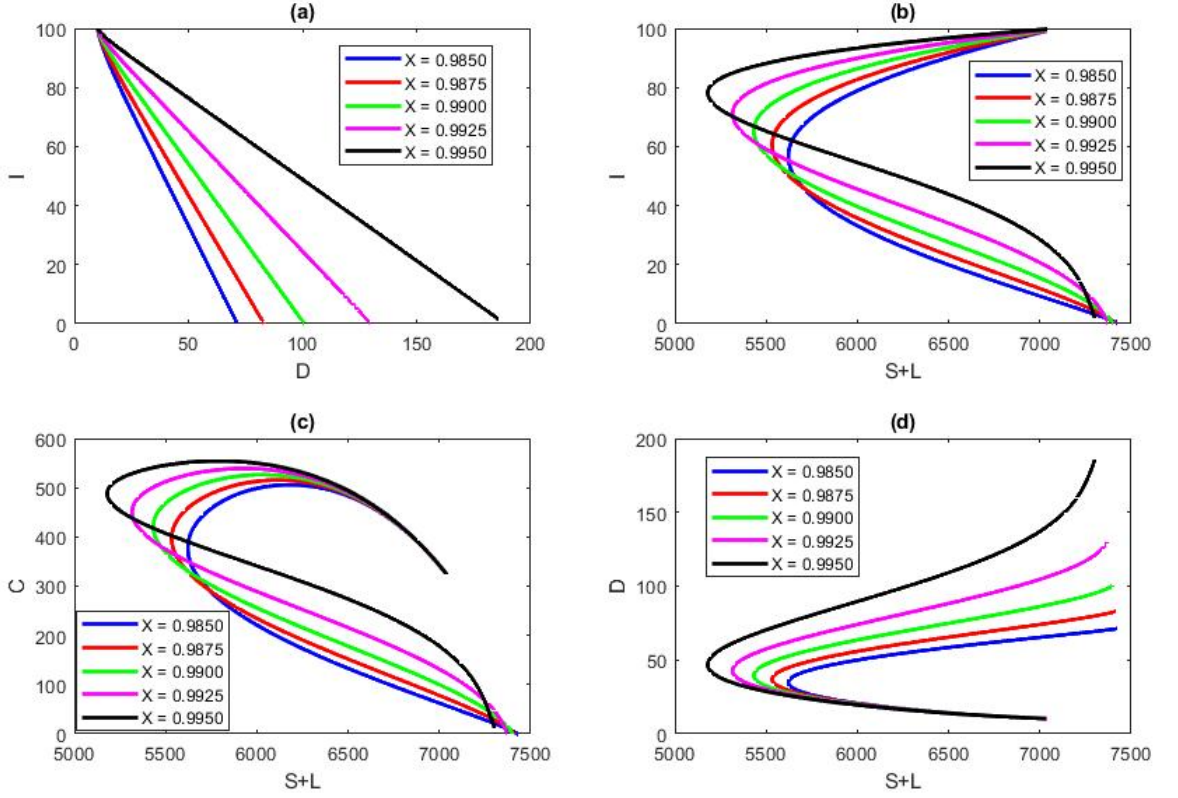


**Fig. 4** Solution of the linearized system (18) with  $X = \beta S_0 / \delta N < 1$ : (a) Phase portrait of  $I(t)$  and  $D(t)$ . (b) Phase portrait of  $I(t)$  and  $S(t) + L(t)$ . (c) Phase portrait of  $C(t)$  and  $S(t) + L(t)$ . (d) Phase portrait of  $D(t)$  and  $S(t) + L(t)$ .

Hence, the next generation matrix  $\mathcal{M}$  [10] and its dominant eigenvalue which is equal to the basic reproduction number  $\mathcal{R}_0$ , are given by

$$\mathcal{M} = -\mathcal{A}\mathcal{B}^{-1} = \begin{pmatrix} \beta S_0 / \delta & 0 \\ 1 & 0 \end{pmatrix}, \quad (21)$$

and

$$\mathcal{R}_0 = \frac{\beta S_0}{\delta N} = \frac{\beta}{\delta} \frac{\nu}{\alpha + \nu} \left(1 - \frac{D_0}{N}\right). \quad (22)$$

Suppose  $D^*$  is the current death toll, then the estimated basic reproduction number  $\mathcal{R}_0^*$  can be expressed as

$$\mathcal{R}_0^* = \frac{\beta}{\delta} \frac{\nu}{\alpha + \nu} \left(1 - \frac{D^*}{N}\right). \quad (23)$$

We can define a lockdown index  $\mathcal{L}$  as

$$\mathcal{L} = \frac{\nu}{\alpha + \nu} < 1, \quad (24)$$

to determine how much the basic reproduction number is reduced due to the lockdown which is the principal investigation of this article. The lockdown index indicates the success and failure of the non-pharmaceutical strategy lockdown.

### 3.6 Stability analysis at $\mathcal{E}_0$

In this section, we discuss the local and global stability of the disease-free equilibrium  $\mathcal{E}_0$  of System (1). We first state:

**Theorem 32** *The disease-free equilibrium  $\mathcal{E}_0$  of System (1) is locally asymptotically stable if  $S_0/N < \rho^{-1}$ , and it is unstable if  $S_0/N > \rho^{-1}$  where  $\rho$  is the basic ratio number defined in (8).*

**Proof.** The characteristic polynomial  $P$  of the linearized system, defined in (18), at the DFE point is

$$P(\lambda) = \det(J(L_0, S_0, I_0, C_0, R_0, D_0) - \lambda I_6). \quad (25)$$

We have the following nonzero eigenvalues of the Jacobian matrix  $J(L_0, S_0, I_0, C_0, R_0, D_0)$  in (17),

$$\lambda_1 = \beta \frac{S_0}{N} - \delta = \left( \frac{\beta S_0}{\delta N} - 1 \right) \delta, \quad \lambda_2 = -(\lambda + \kappa), \quad \lambda_3 = -\gamma, \quad \lambda_4 = -(\alpha + \nu). \quad (26)$$

It follows from (26) that all the eigenvalues are negative if  $\beta S_0/\delta N - 1 < 0$  i.e.  $S_0/N < \rho^{-1}$ , and the eigenvalue  $\lambda_1$  is positive for  $\beta S_0/\delta N - 1 > 0$  i.e.,  $S_0/N > \rho^{-1}$ . All the eigenvalues of the Jacobian matrix  $J(L_0, S_0, I_0, C_0, R_0, D_0)$  are negative implying that  $\mathcal{E}_0$  is locally asymptotically stable. Therefore the disease-free equilibrium  $\mathcal{E}_0$  of system 1 is locally asymptotically stable if  $S_0/N < \rho^{-1}$ , and it is unstable if  $S_0/N > \rho^{-1}$ .  $\square$

Next, in order to establish the global stability analysis at disease-free equilibrium, we construct a Lyapunov function, and we state:

**Theorem 33** *The disease-free equilibrium  $\mathcal{E}_0$  of System (1) is globally asymptotically stable if  $S_0/N < \rho^{-1}$ , and it is unstable if  $S_0/N > \rho^{-1}$ , where  $\rho$  is the basic ratio number defined in (8).*

**Proof.** To show global stability at disease-free equilibrium of the L-SICRD model, considered the following Lyapunov function:

$$G = \frac{1}{8} \delta^2 I^2 - \frac{1}{2} \left( \beta \frac{S_0}{N} - \delta \right) (\lambda + \kappa) C^2, \quad (27)$$

with Lyapunov derivative (where a dot represents differentiation with respect to time) given by

$$\begin{aligned} \dot{G} &= \frac{1}{4} \delta^2 I \dot{I} - \left( \beta \frac{S_0}{N} - \delta \right) (\lambda + \kappa) C \dot{C} \\ &= \frac{1}{4} \delta^2 \left( \beta \frac{S_0}{N} - \delta \right) I^2 - \left( \beta \frac{S_0}{N} - \delta \right) (\lambda + \kappa) C (\delta I - (\lambda + \kappa) C) \\ &= \left( \beta \frac{S_0}{N} - \delta \right) \left( \frac{1}{4} \delta^2 I^2 - \delta (\lambda + \kappa) I C + (\lambda + \kappa)^2 C^2 \right) \\ &= \left( \beta \frac{S_0}{N} - \delta \right) \left( \frac{1}{2} \delta I - (\lambda + \kappa) C \right)^2. \end{aligned} \quad (28)$$

Since all the model parameters and variables (8) are nonnegative (Theorem 31), it follows that  $\dot{G} < 0$  for  $\beta S_0/N - \delta < 0$  i.e.,  $S_0/N < \rho^{-1}$  with  $\dot{G} = 0$  if and only if  $I = C = 0$ . Thus,  $G$  is a Lyapunov function on the domain  $\Omega$ . Therefore, the largest compact invariant subset of  $\Omega$  where  $\dot{G} = 0$  is the subset containing the singleton  $\{(I, C) = (0, 0)\}$ . Thus, it follows, by the LaSalle's invariance principle [19, 26], that

$$(I, C) \rightarrow (0, 0) \quad \text{as } t \rightarrow \infty \quad (29)$$

It follows from (30) that  $\limsup_{t \rightarrow \infty} C = 0$ . Therefore, for sufficiently small  $\varepsilon > 0$ , there exists a constant  $\tau$  such that  $C \leq \varepsilon$  for  $t > \tau$ . Hence the rate of recovered population, the (4th equation of (1)), can be expressed as

$$\frac{dR}{dt} \leq \lambda \varepsilon - \gamma R \quad \text{as } t \rightarrow \infty. \quad (30)$$

Now applying a standard comparison theorem [34], we obtain

$$\limsup_{t \rightarrow \infty} R \leq \frac{\lambda \varepsilon}{\gamma}, \quad (31)$$

again, letting  $\varepsilon \rightarrow 0$ , we get

$$\limsup_{t \rightarrow \infty} R \leq 0. \quad (32)$$

Similarly, one can easily show that

$$\liminf_{t \rightarrow \infty} R \geq 0. \quad (33)$$

From the above two equations, we can conclude that

$$\lim_{t \rightarrow \infty} R = 0. \quad (34)$$

Finally, we obtain that every solution of the model, defined in (1), with initial conditions in the set  $\Omega$ , approaches towards the DFE  $\mathcal{E}_0$  for  $S_0/N < \rho^{-1}$ .  $\square$

### 3.7 Endemic equilibrium

It is obvious that the System (1), always has the endemic equilibrium  $\mathcal{E}_e \in \Omega$  given by

$$\mathcal{E}_e = (L_e, S_e, I_e, C_e, R_e, D_e) = \left( \frac{\alpha\delta}{\beta\nu}N, \frac{\delta}{\beta}N, I_e, \frac{\delta}{\lambda}I_e, \frac{\delta}{\gamma}I_e, D_e \right), \quad (35)$$

where  $D_e$  is the total number of death toll, and it follows from (2) that  $I_e, D_e$  satisfy the equation

$$\left(1 + \frac{\delta}{\lambda} + \frac{\delta}{\gamma}\right)I_e + D_e = \left(1 - \frac{\delta}{\beta} - \frac{\alpha\delta}{\beta\gamma}\right)N. \quad (36)$$

The left hand side of (36) is positive so that the right hand side must be positive. This implies that  $\rho > 1 - \alpha/\nu$ , that is the required condition for endemic equilibrium (EE). For  $I_e = 0$ ,  $\mathcal{E}_0$  and  $\mathcal{E}_e$  coalesce into a single equilibrium. The Jacobian of the EE state is given as:

$$J(L_e, S_e, I_e, C_e, R_e, D_e) = \begin{pmatrix} -a - \alpha - \delta & 0 & \gamma & 0 & \nu \\ a & 0 & 0 & 0 & 0 \\ 0 & \delta & -\lambda & 0 & 0 \\ 0 & 0 & \lambda & -\gamma & 0 \\ 0 & 0 & 0 & 0 & 0 \\ \alpha & 0 & 0 & 0 & -\nu \end{pmatrix}, \quad (37)$$

where we have used  $a := \beta I_e/N$ .

### 3.8 Stability analysis at $\mathcal{E}_e$

In this section, we focus on the local and global stability of the endemic equilibria.

Regarding the local stability, we have to prove that the Jacobian matrix  $J(L_e, S_e, I_e, C_e, R_e, D_e)$  has eigenvalues with negative real parts. This is done by verifying the Routh-Hurwitz conditions.

**Theorem 34** *The endemic equilibrium  $\mathcal{E}_e$  of 1 is locally asymptotically stable if the following conditions hold*

$$\begin{aligned} a_1 &> 0 \quad \text{and} \quad a_4 > 0, \\ a_1 a_2 - a_3 &> 0, \\ a_3(a_1 a_2 - a_3) - a_1^2 a_4 &> 0, \end{aligned} \quad (38)$$

where  $a_1, a_2, a_3$  and  $a_4$  are the coefficients of the equation  $x^4 + a_1 x^3 + a_2 x^2 + a_3 x + a_4 = 0$ .

**Proof.** The characteristic polynomial  $P(\lambda)$  of the linearized system, the corresponding Jacobian matrix is defined in Equation (37), at the EE point is

$$P(\lambda) = \det(J(L_e, S_e, I_e, C_e, R_e, D_e) - \lambda I_6), \quad (39)$$

and the corresponding characteristic equation  $P(\lambda) = 0$  reads

$$\lambda^2(\lambda^4 + a_1\lambda^3 + a_2\lambda^2 + a_3\lambda + a_4) = 0 \quad (40)$$

where

$$\begin{aligned} a_1 &= a + \alpha + \lambda + \gamma + \nu \\ a_2 &= \lambda\gamma + a\nu + a\delta + (\lambda + \gamma)(a + \alpha + \nu) \\ a_3 &= a\nu(\lambda + \gamma) + \lambda\gamma(a + \alpha + \nu) + a\delta(\lambda + \gamma + \nu) \\ a_4 &= a(\lambda\gamma\nu + \lambda\delta\nu + \gamma\nu\delta). \end{aligned} \quad (41)$$

The endemic equilibrium  $\mathcal{E}_e$  is locally asymptotically stable if the real part of all non-zero eigenvalues are negative. The Routh-Hurwitz theorem states that all the roots of (40) have negative real parts iff

$$\Delta_i > 0, \text{ for } i = 1, \dots, 4, \quad (42)$$

where

$$\Delta_1 = a_1, \quad \Delta_2 = \begin{vmatrix} a_1 & a_3 \\ 1 & a_2 \end{vmatrix}, \quad \Delta_3 = \begin{vmatrix} a_1 & a_3 & 0 \\ 1 & a_2 & a_4 \\ 0 & a_1 & a_3 \end{vmatrix}, \quad \Delta_4 = \begin{vmatrix} a_1 & a_3 & 0 & 0 \\ 1 & a_2 & a_4 & 0 \\ 0 & a_1 & a_3 & 0 \\ 0 & 1 & a_2 & a_4 \end{vmatrix}.$$

The conditions defined in (38) and (43) are identical, which completes the proof.  $\square$

We next focus on the global stability at  $\mathcal{E}_e$  construct a Lyapunov function to verify the endemic equilibrium.

**Theorem 35** *The endemic equilibrium  $\mathcal{E}_e$  of System (1) is globally asymptotically stable if  $I/S \leq c(\alpha/\delta)$  where  $c$  is a positive constant.*

**Proof.** To solve the system (1), for an endemic equilibrium  $\mathcal{E}_e \in \Omega$ , followed from (35), we first notice that

$$\begin{aligned} \alpha S_e &= \nu L_e, \\ \delta I_e &= \lambda C_e = \gamma R_e. \end{aligned} \quad (43)$$

Therefore, we obtain

$$\alpha = \frac{Q}{S_e}, \quad \nu = \frac{Q}{L_e}, \quad \delta = \frac{P}{I_e}, \quad \lambda = \frac{P}{C_e}, \quad \gamma = \frac{P}{R_e}, \quad (44)$$

where  $P$  and  $Q$  are two positive constants. We construct the following nonlinear Lyapunov function:

$$V = S - S_e - S_e \ln\left(\frac{S}{S_e}\right) + I - I_e - I_e \ln\left(\frac{I}{I_e}\right) + C - C_e - C_e \ln\left(\frac{C}{C_e}\right) + R - R_e - R_e \ln\left(\frac{R}{R_e}\right) + L - L_e - L_e \ln\left(\frac{L}{L_e}\right). \quad (45)$$

We define two functions  $G$  and  $g$  such that

$$\begin{aligned} G &= S - S_e - S_e \ln\left(\frac{S}{S_e}\right) \\ &= S_e \left[ \frac{S}{S_e} - 1 - \ln\left(\frac{S}{S_e}\right) \right] \\ &= S_e g\left(\frac{S}{S_e}\right), \end{aligned}$$

where  $g : x \mapsto x - 1 - \ln(x)$ . It is easy to verify that  $g(x) \geq 0$ , for all  $x \in [0, \infty)$  and  $g(x) = 0$  if and only if  $x = 1$ . Thus, the function  $V(t) \geq 0$  and  $V(t) = 0$ , if and only if  $S = S_e$ ,  $I = I_e$ ,  $C = C_e$ ,  $R = R_e$ ,  $L = L_e$ . Differentiating  $V(t)$  with respect to  $t$  and using (1) and (44), we obtain

$$\begin{aligned}
\dot{V} &= \dot{S} - \frac{S_e}{S} \dot{S} + \dot{I} - \frac{I_e}{I} \dot{I} + \dot{C} - \frac{C_e}{C} \dot{C} + \dot{R} - \frac{R_e}{R} \dot{R} + \dot{L} - \frac{L_e}{L} \dot{L} \\
&= \left(1 - \frac{S_e}{S}\right) \left[ -(P+Q) \frac{S}{S_e} - P \frac{I}{I_e} + P \frac{R}{R_e} + Q \frac{L}{L_e} \right] \\
&\quad + \left(1 - \frac{I_e}{I}\right) P \frac{S}{S_e} + \left(1 - \frac{C_e}{C}\right) P \left[ \frac{I}{I_e} - \frac{C}{C_e} \right] \\
&\quad + \left(1 - \frac{R_e}{R}\right) P \left[ \frac{C}{C_e} - \frac{R}{R_e} \right] + \left(1 - \frac{L_e}{L}\right) Q \left[ \frac{S}{S_e} - \frac{L}{L_e} \right] \\
&= P \left[ 3 + \frac{S_e I}{S I_e} - \frac{S_e R}{S R_e} - \frac{I_e S}{I S_e} - \frac{C_e I}{C I_e} - \frac{R_e C}{R C_e} \right] \\
&\quad + Q \left[ 2 - \frac{S_e L}{S L_e} - \frac{L_e S}{L S_e} \right].
\end{aligned} \tag{46}$$

Since the arithmetic mean exceeds the geometric mean, we have

$$\begin{aligned}
\left[ 4 - \frac{S_e R}{S R_e} - \frac{I_e S}{I S_e} - \frac{C_e I}{C I_e} - \frac{R_e C}{R C_e} \right] &\leq 0, \\
\left[ 2 - \frac{S_e L}{S L_e} - \frac{L_e S}{L S_e} \right] &\leq 0.
\end{aligned} \tag{47}$$

Therefore, we obtain  $\dot{V} = 0$  if and only if  $S = S_e$ ,  $I = I_e$ ,  $C = C_e$ ,  $R = R_e$  and  $L = L_e$ , and  $\dot{V} < 0$  for  $S_e I / (S I_e) \leq 1$  i.e.  $I/S \leq (P/Q)(\alpha/\delta) = A(\alpha/\delta)$ .  $\square$

## 4 Numerical experiments

In this section, we derive the error function to estimate the model parameters using available data [1, 2, 5] and MATLAB minimizing function `fminsearch`. In addition, we analyze the epidemic results calculated for Canada and the three most populated provinces, Ontario, Québec and British Columbia which were the most affected by the COVID-19. We compare the calculated outcomes with the available data [1, 2, 5] for the so called *first wave*, a period of 168 days, from January 25, 2020 to July 10, 2020.

### 4.1 Model parameter estimation

We focus on the exponential growth phase of the COVID-19 epidemic in Canada, as well as the provinces which were the most significantly affected by the coronavirus. The time resolved (daily updated) database [1, 2, 5] provides the number of corona-positive cases, the number of recovered and the number of deaths. The optimal values of  $\mathbf{p} = (q_1, q_2, \alpha, \beta, \gamma, \delta, \lambda, \kappa, \nu)^T$ , that is the set of initial value adjusting and model parameters, is obtained by minimizing the root mean square error function  $E(\mathbf{p})$ , defined as

$$E(\mathbf{p}) = \frac{1}{M} \sqrt{\sum_{i=1}^M (T_i - \tilde{T}_i)^2 + (R_i - \tilde{R}_i)^2 + (D_i - \tilde{D}_i)^2}, \tag{48}$$

where  $\tilde{T}_i$ ,  $\tilde{R}_i$  and  $\tilde{D}_i$  are the publicly available data of total cases, total recovered and total deaths on the particular  $i$ th day, and  $T_i (= C_i + R_i + D_i)$ ,  $R_i$  and  $D_i$  are the calculated results obtained from the system (1). We have denoted by  $M$  is the size of the data set, and  $C_i$  is the total corona-positive cases on the  $i$ th day. To minimize the error function we employ the MATLAB function `fminsearch` for myriad number of iterations.

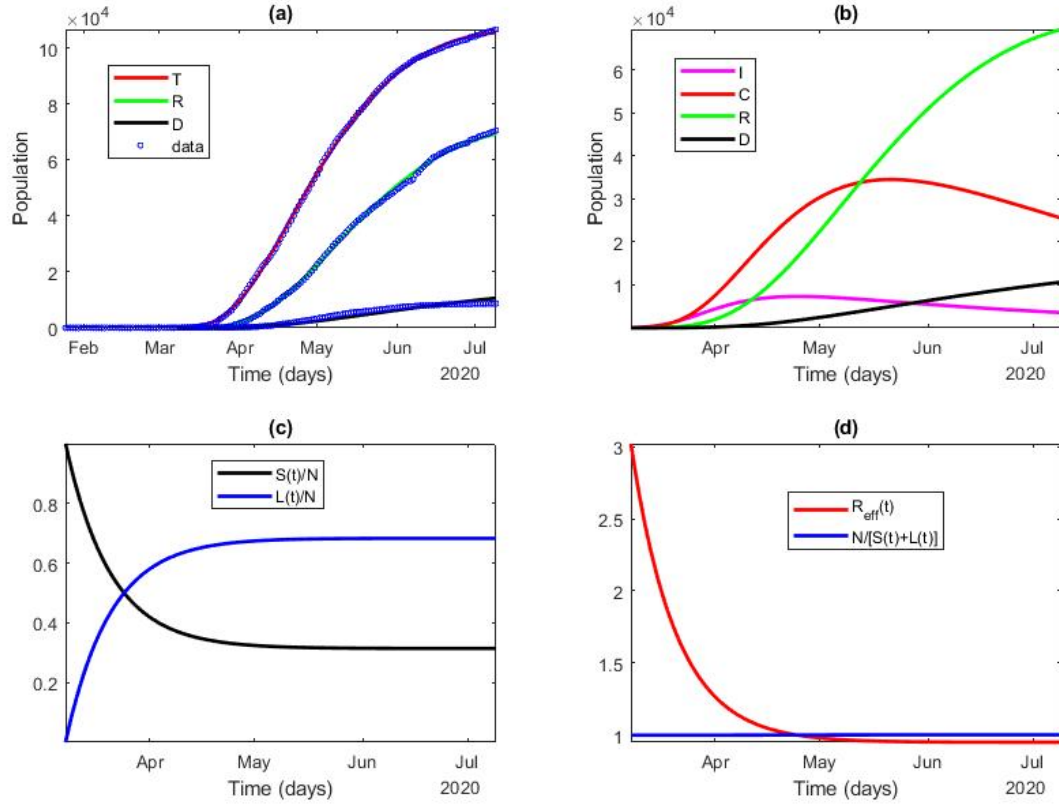


**Fig. 5 Model Calculation for Canada :** (a) Estimation of the total number of coronavirus cases ( $T$ ), the total number of recovered ( $R$ ) and total number of deaths ( $D$ ) compared to the available data [2]. (b) Model calculation of the population related to the COVID-19. Here  $I, C, R, D$  represent the group of infected persons, the corona-positive cases, recovered and deaths, respectively. (c) Estimation of the number of susceptible individuals  $S(t)/N$  and of the number of lockdown individuals  $L(t)/N$ . (d) Effective reproduction function compared to the quantity  $N/(S(t) + L(t))$  which varies near the unity.

**Table 1** The initial values of the model compartments and starting time  $t_0$  (Day 1) from Subsection 2.1, for Canada and three of its provinces, Ontario, Québec and British Columbia.

Parameters	Canada	Ontario	Québec	British Columbia
$L(t_0)$	7	24	33	4
$S(t_0)$	37894668	14711736	8537180	5110852
$I(t_0)$	57	25	367	34
$C(t_0)$	58	36	92	22
$R(t_0)$	8	5	1	4
$D(t_0)$	1	1	1	1
$t_0$	Mar. 08, 2020	Mar. 11, 2020	Mar. 18, 2020	Mar. 08, 2020

## 4.2 Results and Discussions

The initial values of the model compartments, lockdown, susceptible, infected, corona-positive cases, recovered and deaths, and starting time  $t_0$  (Day 1), mentioned in Subsection 2.1, for Canada and three of its provinces, Ontario, Québec and British Columbia are presented in Table 1. To get a better estimate, we consider the starting time  $t_0$  such that the initial value of the death compartment,  $D(t_0)$ , is nonzero.

The estimated values of the model parameters,  $q_1, q_2, \alpha, \beta, \gamma, \delta, \lambda, \kappa$  and  $\nu$ , for Canada and three provinces, Ontario, Québec and British Columbia, are presented in Table 2.

The values of the error function  $E(\mathbf{p})$ , basic ratio  $\rho$ , lockdown index  $\mathcal{L}$ , estimated basic reproduction number  $\mathcal{R}_0^*$  for Canada and three of its provinces, Ontario, Québec and British Columbia are presented

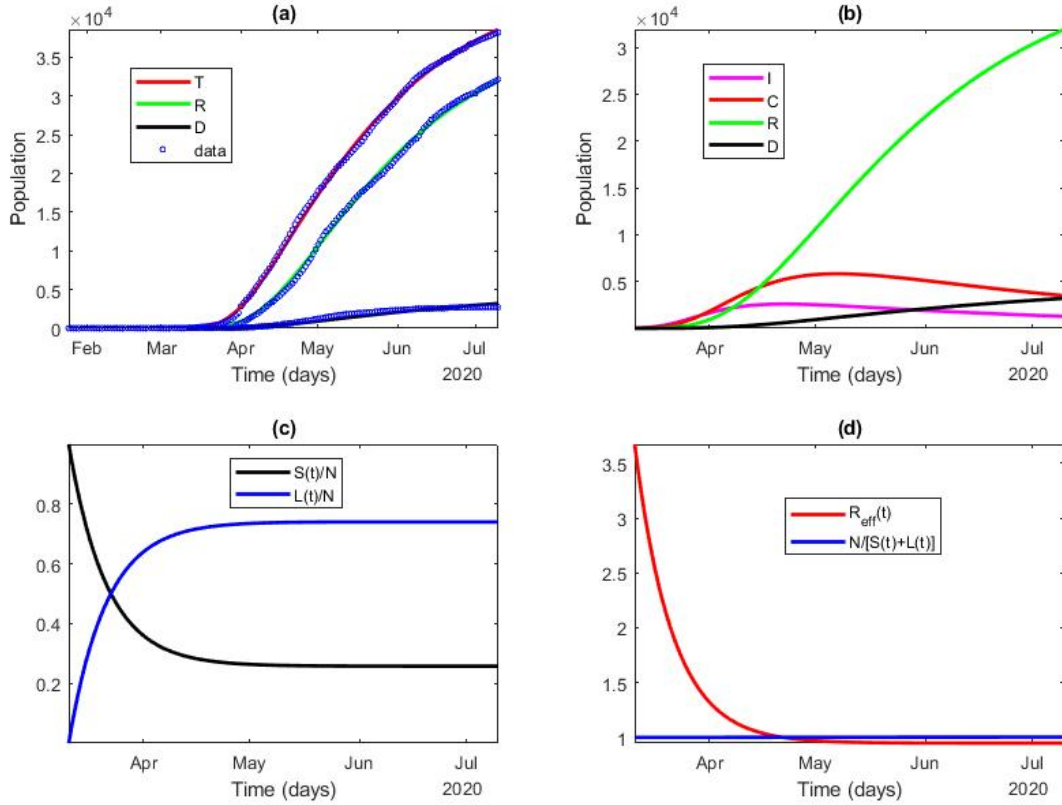


**Fig. 6 Model Calculation for Ontario :** (a) Estimation of the total number of coronavirus cases ( $T$ ), the total number of recovered ( $R$ ) and total number of deaths ( $D$ ) compared to the available data [5]. (b) Model calculation of the population related to the COVID-19. Here  $I, C, R, D$  represent the group of infected persons, the corona-positive cases, recovered and deaths, respectively. (c) Estimation of the number of susceptible individuals  $S(t)/N$  and of the number of lockdown individuals  $L(t)/N$ . (d) Effective reproduction function compared to the quantity  $N/(S(t) + L(t))$  which varies near the unity.

**Table 2** The estimated values of the model parameters from Subsection 2.2, for Canada and three provinces, Ontario, Québec and British Columbia.

Parameters	Canada	Ontario	Québec	British Columbia
$q_1$	0.98227377	0.69984435	3.98585365	1.54494093
$q_2$	0.12429425	0.66989657	0.36078469	0.16310273
$\alpha$	0.05356217	0.07001473	0.01433872	0.16504446
$\beta$	0.75378015	0.77531374	0.56851456	0.76464980
$\gamma$	0.01182917	0.00380846	0.00611318	0.00102500
$\delta$	0.24959578	0.21111558	0.40733442	0.21344721
$\lambda$	0.04059485	0.08073105	0.01516258	0.06260813
$\kappa$	0.00376294	0.00668845	0.00306512	0.00412335
$\nu$	0.02462661	0.02436737	0.02489909	0.05557474

in the Table 3. Small lockdown index suggests that a large number of people are following the lockdown policy. Table 3 shows that lockdown index of Québec is significantly higher than that of Ontario, British Columbia and Canada. However, the basic ratio of Québec is appreciably lower than that of Ontario, British Columbia and Canada which indicates that either incubation period in Québec is very short or a high volume of procedures for corona test is underway in Québec. The latter may be the possible reason, as the testing procedure separates corona-positive cases from the population, preventing the spread of the disease. The estimated basic reproduction number is less than one for Canada and its three provinces which specifies that the outbreak is under control.

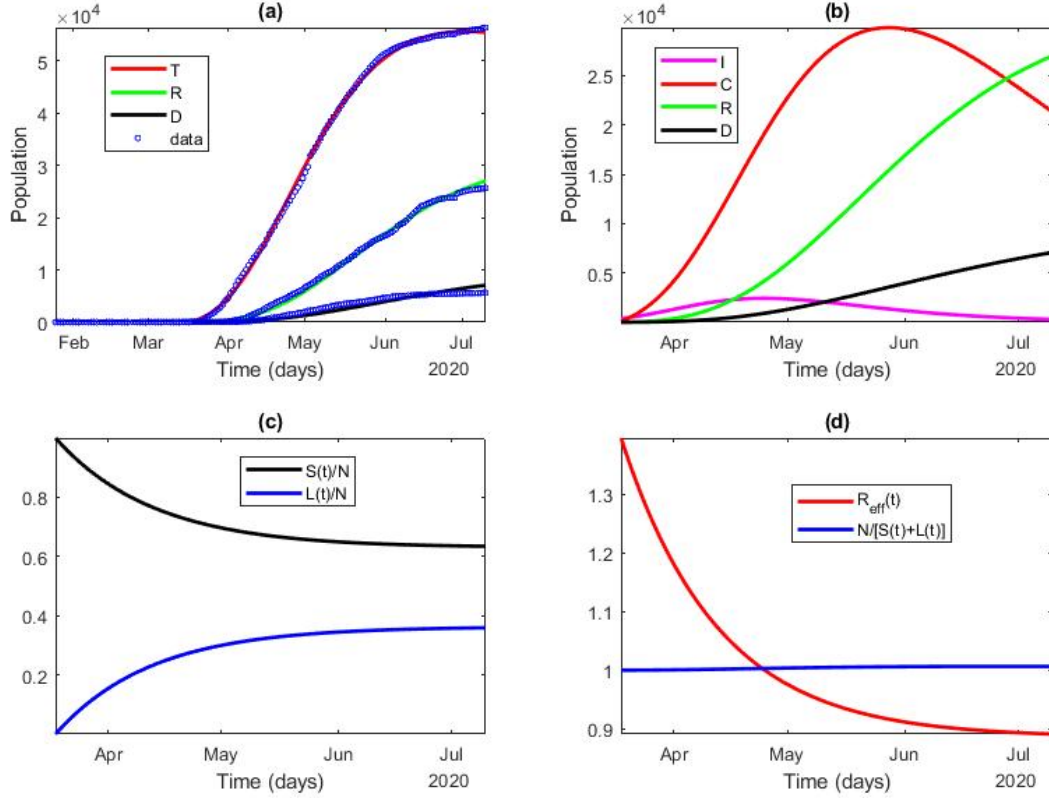


**Fig. 7 Model Calculation for Québec:** (a) Estimation of the total number of coronavirus cases ( $T$ ), the total number of recovered ( $R$ ) and total number of deaths ( $D$ ) compared to the available data [5]. (b) Model calculation of the population related to the COVID-19. Here  $I, C, R, D$  represent the group of infected persons, the corona-positive cases, recovered and deaths, respectively. (c) Estimation of the number of susceptible individuals  $S(t)/N$  and of the number of lockdown individuals  $L(t)/N$ . (d) Effective reproduction function compared to the quantity  $N/(S(t) + L(t))$  which varies near the unity.

**Table 3** The values of the error function  $E(\mathbf{p})$ , basic ratio  $\rho$ , lockdown index  $\mathcal{L}$ , estimated basic reproduction number  $\mathcal{R}_0^*$  for Canada and three provinces, Ontario, Québec and British Columbia.

Parameters	Canada	Ontario	Québec	British Columbia
$E(\mathbf{p})$	107.51698976	49.67222853	92.91585716	8.33570694
$\rho$	3.02000356	3.67246111	1.39569487	3.58238360
$\mathcal{L}$	0.31496350	0.25817786	0.63456875	0.25190347
$\mathcal{R}_0^*$	0.95097128	0.94797078	0.88508218	0.90238186

The estimated values of the model variables such as susceptible, corona-positive cases etc. for Canada are presented in Figure 5 along with the available data [2]. Figure 5(a) shows that the total number of coronavirus cases, the number of recovered individuals and the total deaths, are in perfect agreement with the data [2]; the value of the relative error is approximately 0.001. The model calculations of the population for infected group ( $I$ ), corona-positive cases ( $C$ ), recovered ( $R$ ) and deaths ( $D$ ) are presented in Figure 5(b). The diagram shows that the number of current daily corona-positive cases is significantly low compared to the daily recovery number, and the daily death number is relatively low. Figure 5(c) shows that the number of susceptible individuals  $S(t)/N$  is less compared to the number of individuals in lockdown  $L(t)/N$ , which implies that people keep themselves safe and as a result the outbreak is going over. Figure 5(d) shows that the epidemic is under control; initially the curve  $R_{eff}(t)$  was above the curve  $N/(S(t) + L(t))$ , varying close to unity, but latter is gradually decreasing and currently below the curve  $N/(S(t) + L(t))$ .



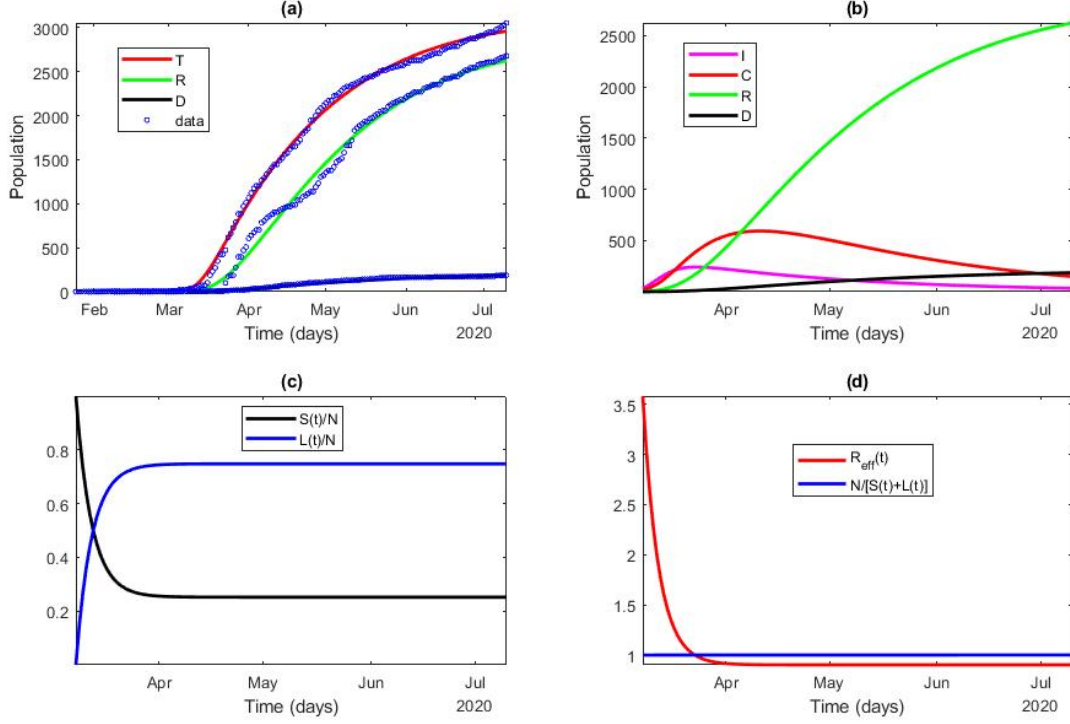


**Fig. 8 Model Calculation for British Columbia:** (a) Estimation of the total number of coronavirus cases ( $T$ ), the total number of recovered ( $R$ ) and total number of deaths ( $D$ ) compared to the available data [5]. (b) Model calculation of the population related to the COVID-19. Here  $I, C, R, D$  represent the group of infected persons, the corona-positive cases, recovered and deaths, respectively. (c) Estimation of the number of susceptible individuals  $S(t)/N$  and of the number of lockdown individuals  $L(t)/N$ . (d) Effective reproduction function compared to the quantity  $N/(S(t) + L(t))$  which varies near the unity.

The estimated values of the model variables such as susceptible, corona-positive cases etc. for Ontario are presented in Figure 6 along with the available data [5]. The epidemically picture of Ontario is almost similar to the one of Canada, except for the quantitative values. Figure 6(a) shows that the total number of coronavirus cases ( $T$ ), the total number of recovered ( $R$ ) and the estimated number of deaths, are in perfect agreement with the data [5]; the value of the relative error is approximately 0.0011. The model calculations of the population for infected group ( $I$ ), corona-positive cases ( $C$ ), recovered ( $R$ ) and deaths ( $D$ ) are presented in Figure 6(b). The diagram shows that the number of current daily corona-positive cases is significantly low compared to the daily recovery number, while the daily death number is relatively low. Figure 6(c) shows that the number susceptible individuals  $S(t)/N$  is less compared to the number of lockdown individuals  $L(t)/N$ , which implies that people keep themselves safe and as a consequence the outbreak is going over. Figure 6(d) shows that the epidemic is under control; initially the curve  $R_{eff}(t)$  was above the curve  $N/(S(t) + L(t))$ , varying close to unity, but latter is gradually decreasing and currently below the curve  $N/(S(t) + L(t))$ .

The estimated values of the model variables such as susceptible, corona-positive cases etc. for Québec are presented in Figure 7 along with the available data [5]. The picture of COVID-19 in this province is slightly different than in the other provinces of Canada. Figure 7(a) shows that the results calculated for the total number of coronavirus cases ( $T$ ), the total number of recovered individuals ( $R$ ) and the estimated number of deaths ( $D$ ) are in good agreement with the data [5]; the value of the relative error is approximately 0.0017. The model calculations of the population for infected group ( $I$ ) corona-positive cases ( $C$ ), recovered ( $R$ ) and deaths ( $D$ ) are presented in Figure 7(b). The diagram shows that the number of corona-positive cases and the number of deaths are higher in Québec compared to the other provinces. Figure 7(c) shows that the curves of susceptible individuals  $S(t)/N$  and individuals in lockdown  $L(t)/N$  are parallel to the time axis and susceptible individuals  $S(t)/N$  are higher compared to the number of lockdown individuals  $L(t)/N$ . This implies that some people keep themselves safe and as a consequence

the outbreak is also going over. Figure 7(d) shows that the epidemic is under control; initially the curve  $R_{\text{Eff}}(t)$  was above the curve  $N/(S(t) + L(t))$ , varying close to unity, but latter is gradually decreasing and currently below the curve  $N/(S(t) + L(t))$ .

The estimated values of the model variables such as susceptible, corona-positive cases etc. for British Columbia are presented in Figure 8 along with the available data [5]. Figure 8(a) shows that the total number of coronavirus cases ( $T$ ), of recovered people and the estimated number of deaths are in good agreement with the data [5]; the value of the relative error is approximately 0.0027. The model calculations of the population for infected group ( $I$ ), corona-positive cases ( $C$ ), recovered ( $R$ ) and deaths ( $D$ ) are presented in Figure 8(b). The diagram shows that the number of current corona-positive cases is significantly lower compared to the number of recovered individuals, and the daily death number is not high. Figure 8(c) shows that susceptible individuals  $S(t)/N$  are less compared to the number of individuals in lockdown  $L(t)/N$ . This implies that people keep themselves safe and as a consequence the outbreak is also going over. Figure 8(d) shows that the epidemic is under control; initially the curve  $R_{\text{Eff}}(t)$  was above the curve  $N/(S(t) + L(t))$ , varying close to unity, but latter is gradually decreasing and currently below the curve  $N/(S(t) + L(t))$ .

## 5 Improvement of the model

In this section we propose different possible refinements and improvements of the model, including spatial dependence, partial inter-provincial lockdown, and “at risk” vs healthy populations. Finally an optimization procedure is introduced to analyze different scenarios. Some experiments will also be proposed to illustrate the proposed improvements.

### 5.1 Spatial dependence

The system of equations (1) allows for an accurate modeling of the spread of disease in Canada or in a given province. We here propose a generalization of the model considering a coupling of  $P$  systems, each one modeling the spread in a given province. We denote by  $\mathbf{p}_k = (\alpha_k, \beta_k, \gamma_k, \delta_k, \lambda_k, \kappa_k, \nu_k)^T$  (resp.  $\mathbf{Y}_k = (S_k, I_k, Q_k, R_k, D_k, L_k)^T$ ) the set of parameters (resp. unknowns) in Province  $k \in \{1, \dots, P\}$ . We denote by  $N_k$  the total population in Province  $k$ , and we have  $N = \sum_{k=1}^P N_k$  the total population in Canada. The objective is now to consider the evolution in each province considering population migration between provinces. We consider for each  $k \in \{1, \dots, P\}$

$$\frac{d\mathbf{Y}_k}{dt} = \mathcal{F}_k(\mathbf{Y}_k), \quad (49)$$

where the function  $\mathcal{F}_k$  reads

$$\mathcal{F}_k(\mathbf{Y}_k) = \mathbf{A}_k \mathbf{Y}_k + \mathbf{F}_k, \quad (50)$$

with  $\mathbf{Y}_k(0) = \mathbf{Y}_k^0 \in \mathbb{R}^6$  and  $\mathbf{F}_k = (-\beta_k/N_k, \beta_k/N_k, 0, \dots, 0)^T S_k I_k$ , where  $\mathbf{p}_k$  is time-independent,  $\mathbf{F}_k$  and  $N_k$  is time-dependent such that  $\sum_{k=1}^P N_k(t) = N$  is constant. Finally, we have

$$\mathbf{A}_k = \begin{pmatrix} -\alpha_k & 0 & 0 & \gamma_k & 0 & \nu_k \\ 0 & -\delta_k & 0 & 0 & 0 & 0 \\ 0 & \delta_k & -(\lambda_k + \kappa_k) & 0 & 0 & 0 \\ 0 & 0 & \lambda_k & -\gamma_k & 0 & 0 \\ 0 & 0 & \kappa_k & 0 & 0 & 0 \\ \alpha_k & 0 & 0 & 0 & 0 & -\nu_k \end{pmatrix}.$$

We denote by  $\mathbf{Y}_k^n$  the approximate solution to (51) at time  $t_n$  for  $n \in \{0, \dots, M\}$ .

$$\mathbf{Y}_k^{n+1} = \mathbf{Y}_k^n + \mathbf{A}_k \int_{t_n}^{t_{n+1}} \mathbf{Y}_k(s) + \mathbf{F}_k(s) ds, \quad (51)$$

For each  $k \in \{1, \dots, P\}$

$$E(\mathbf{p}_k) = \frac{1}{M} \sqrt{\sum_{n=1}^M \|\mathbf{Y}_k^n - \bar{\mathbf{Y}}_k(t_n)\|_2^2}, \quad (52)$$

where  $\bar{\mathbf{Y}}_k(t_n)$  are the given data available in Province  $k$  and time  $t_n$ . If there is *no population migration*, the parameters  $\mathbf{p}_k$ 's are all computed independently. More importantly, during the “parameterization” of the model, we perform computation using the existing data, independently for any  $k \in \{1, \dots, P\}$ . This is performed from iterations from 0 to  $M$ .

Now, if *population migration* is allowed between provinces for  $t \geq t_M$ , we propose the following approach. We denote by  $\mathcal{S}(t)$  a stochastic matrix (for all  $j \in \{1, \dots, P\}$ ,  $\sum_{i=1}^P \mathcal{S}_{ij}(t) = 1$ ) defined as follows

$$\mathcal{S}_{ij}(t) = \begin{cases} \sigma_{ij}(t), & j \neq i, \\ 1 - \sum_{j \neq i} \sigma_{ji}(t), & j = i. \end{cases}$$

When coefficients  $\sigma_{ij}$  are null, there is no population migration between provinces (inter-provincial lockdown) and the  $P$  systems are totally decoupled. We then represent Canada as a complete graph of  $P$  nodes and  $P(P-1)/2$  edges. For a given Province  $k$ , the coefficient  $0 < \sigma_{kj} < 1$  models the population moving to Province  $j$ . The stochastic matrix  $\mathcal{S}$  are hence controlled by provincial governments. Hence,  $\sigma_{kj} = 0$  if Province  $j$  does not allow migration from Province  $k$ . In practice, those daily coefficients are close to 0. This approach allows for a simple and cheap way to model spatial dependence without explicitly introduce a spatial variable in the model. From a practical point of view, we also assume that only *susceptible (S)*, *infected (I) spreading the contagious disease* and *recovered (R)* individuals are susceptible to cross the borders. We then define the set of susceptible, infected, and recovered in every provinces:  $\mathbf{S} = [S_1, \dots, S_P]^T$ ,  $\mathbf{I} = [I_1, \dots, I_P]^T$ , and  $\mathbf{R} = [R_1, \dots, R_P]^T$ . We then define, some stochastic matrices for each category:  $\mathcal{S}_S^n := \mathcal{S}_S(t_n)$ ,  $\mathcal{S}_I^n := \mathcal{S}_I(t_n)$ , and  $\mathcal{S}_R^n := \mathcal{S}_R(t_n)$ , where for  $\mathcal{S}_{C,D,L}^n = Id \in \mathbb{R}^{P \times P}$ . Then, population migration is modeled as follows at each time iteration  $n$ :  $\mathbf{S}^n \rightarrow \mathcal{S}_S^n \mathbf{S}^n$ ,  $\mathbf{I}^n \rightarrow \mathcal{S}_I^n \mathbf{I}^n$ , ... In the following, the indices S,I,R correspond to 1,2,4, and C,D,L correspond to 3,5,6. We propose the following modeling. For each province, we compute

$$\tilde{\mathbf{Y}}_k^{n+1} = \mathbf{Y}_k^n + A_k \int_{t_n}^{t_{n+1}} \mathbf{Y}_k(s) + \mathbf{F}_k(s) ds.$$

with for province  $k$ ,  $\mathbf{Y}_k^{n+1} = \{Y_{k;\ell}^{n+1}\}_{\ell=1,\dots,6}$  defined as follows

$$Y_{k;\ell}^{n+1} = \sum_{i=1}^P \mathcal{S}_{\ell;(k,i)}^{n+1} \tilde{Y}_{i;\ell}^{n+1}. \quad (53)$$

If  $\ell = 3, 5, 6$ , then for all  $k \in \{1, \dots, P\}$  we have  $Y_{k;\ell}^{n+1} = \tilde{Y}_{k;\ell}^{n+1}$ . Moreover  $N_k^{n+1} = \|\mathbf{Y}_k^{n+1}\|_1 = \sum_{\ell=1}^6 |Y_{k;\ell}^{n+1}|$ , and we denote  $\mathbf{N}^n = [N_1^n, \dots, N_P^n]^T$ . The algorithm is summarized in Algo. 5.1.

**Proposition 51** *For all  $n \geq 0$  in Algorithm 5.1, we have  $\|\mathbf{N}^n\|_\ell = N$ .*

**Proof.** Assume that at iteration the statement is true. At iteration  $n+1$ , and by construction, we have

$$\sum_{k=1}^P \|\tilde{\mathbf{Y}}_k^{n+1}\|_1 = \sum_{k=1}^P \sum_{\ell=1}^6 \tilde{Y}_{k;\ell}^{n+1} = N.$$

Hence, from

$$\begin{aligned} \|\mathbf{N}^{n+1}\|_1 &= \sum_{k=1}^P N_k^{n+1} \\ &= \sum_{k=1}^P \sum_{\ell=1}^6 Y_{k;\ell}^{n+1} \\ &= \sum_{k=1}^P \sum_{\ell=1}^6 \sum_{i=1}^P \mathcal{S}_{\ell;(k,i)}^{n+1} \tilde{Y}_{i;\ell}^{n+1} \\ &= \sum_{\ell=1}^6 \sum_{i=1}^P \tilde{Y}_{i;\ell}^{n+1} \sum_{k=1}^P \mathcal{S}_{\ell;(k,i)}^{n+1}. \end{aligned}$$

We recall that  $\sum_{k=1}^P \mathcal{S}_{\ell;(k,i)}^{n+1} = 1$  for any  $i \in \{1, \dots, P\}$  and any  $\ell \in \{1, \dots, 6\}$  as the matrices  $\mathcal{S}$  are stochastic. Thus

$$\|\mathbf{N}^{n+1}\|_1 = \sum_{k=1}^P N_k^{n+1} = \sum_{\ell=1}^6 \sum_{i=1}^P \tilde{Y}_{i;\ell}^{n+1} = N.$$

This concludes the proof.  $\square$

This proposition confirms the consistency of the multi-province model, using stochastic matrices.

---

**Algorithm 1** Coronavirus spread in multi-province modeling

---

1: Minimize the following functional

$$E(\mathbf{p}_k^M) = \frac{1}{M} \sqrt{\sum_{n=1}^M \|\mathbf{Y}_k^n - \bar{\mathbf{Y}}_k(t_n)\|_2^2}.$$

where for  $0 \leq n \leq M$ ,  $\mathbf{Y}_k^n$ , solution to

$$\mathbf{Y}_k^{n+1} = \mathbf{Y}_k^n + A_k \int_{t_n}^{t_{n+1}} \mathbf{Y}_k(s) + \mathbf{F}_k(s) ds.$$

2: For any  $n \in \{M, \dots, \mathcal{M}\}$  and for all  $k \in \{1, \dots, P\}$ , compute

$$\tilde{\mathbf{Y}}_k^{n+1} = \mathbf{Y}_k^n + A_k \int_{t_n}^{t_{n+1}} \mathbf{Y}_k(s) + \mathbf{F}_k(s) ds.$$

- Define stochastic matrices  $\mathcal{S}_\ell$  for  $\ell = 1, 2, 4$  to model population migration.
- Update the solution, for all  $k \in \{1, \dots, P\}$ :

$$Y_{k;\ell}^{n+1} = \sum_{i=1}^P \mathcal{S}_{\ell;(k,i)}^{n+1} \tilde{Y}_{i;\ell}^{n+1}.$$


---

## 5.2 Provincial lockdown

In this subsection, we discuss population migration between provinces. The total population in Province indexed by  $k$  at time  $t_n$ , is denoted by  $N_k^n = N_k(t_n)$ . We will assume below that international borders are closed so that the total population  $\sum_{k=1}^P N_k^n = N$  is a constant. If we assume that inter-provincial migration is allowed, independently of the disease. In this case the stochastic matrix is “full”. **Whenever inter-province migration is forbidden, the stochastic matrix is the identity matrix.** We assume initially that  $N_{AL}^0 = 4.371 \times 10^6$  (Alberta),  $N_{BC}^0 = 5.071 \times 10^6$  (British Columbia),  $N_{ON}^0 = 14.57 \times 10^6$  (Ontario), and  $N_{QC}^0 = 8.485 \times 10^6$  (Québec).

**Standard migration.** Daily, we assume that up to 0.5% of the population of BC and Alberta provinces are susceptible to move to another province. Similarly 0.125% (resp. 0.17%) of the Ontario (resp. Québec) province are susceptible to move to another province. Let us show after 150 days the total population without provincial lockdown. We report in Fig. 9 (Left) the total variation of the population in each province over the period of 150 days, and in Fig. 9 (Right) the daily variations. This experiment shows that inter-provincial migration has a long-term effect on the province population.

**Partial migration/inter-provincial lockdown.** We assume that between day 50 and 100, the province of Ontario reduces by 90% the entries at its border to all the other provinces, and that only Québec and B.C. do the same only for Ontario. The other provinces continue to receive individuals from Ontario. This experiment illustrates the effect of provincial lockdown policies among provinces. This is naturally a crucial criterium to control the disease.

**Inter-provincial lockdown.** In this experiment, we study the case of 2 provinces, Ontario and Québec, assuming that initially only one province (Québec) is mainly affected by the COVID-19. We then consider 3 situations, full inter-provincial lockdown, partial inter-provincial lockdown, and open borders. We

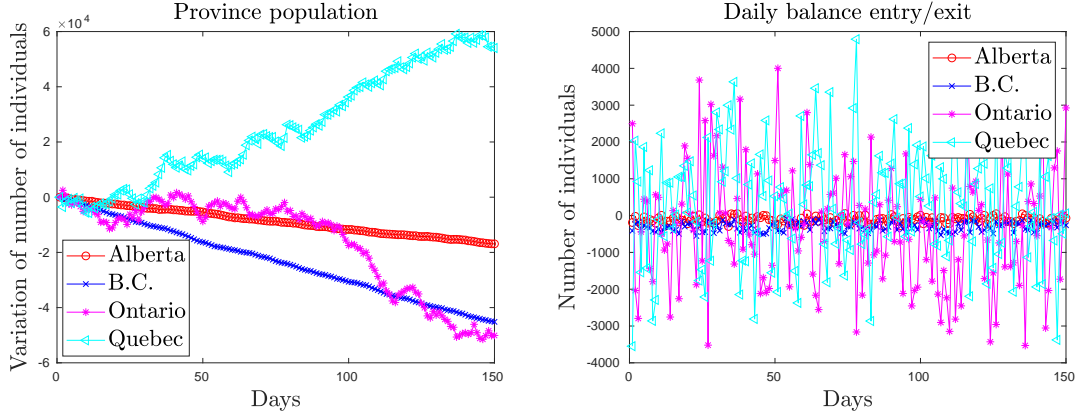


**Fig. 9 Standard migration.** (Left) Total variation of population in each province (Right) Daily variation.

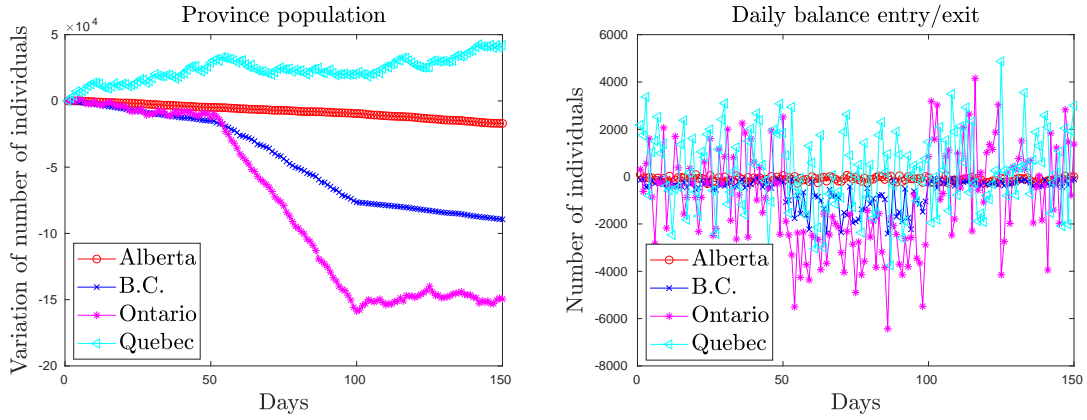


**Fig. 10 Partial migration/inter-provincial lockdown.** (Left) Total variation of population in each province (Right) Daily variation.

denote by  $\mathbf{Y}_{\text{ON}}$ ,  $\mathbf{Y}_{\text{QC}}$  the Ontario and Québec province variables. The numerical system reads

$$\begin{cases} \tilde{\mathbf{Y}}_{\text{ON},\text{QC}}^{n+1} = \mathcal{F}_{\text{ON},\text{QC}}(\mathbf{Y}_{\text{ON},\text{QC}}^n) \\ \mathbf{Y}_{k;\ell}^{n+1} = \sum_{i=1}^2 \mathcal{S}_{\ell;(k,i)}^{n+1} \tilde{\mathbf{Y}}_{i;\ell}^{n+1} \end{cases}$$

Initially, we assume that

- In Ontario:  $I^0 = 5$ ,  $C^0 = 5$ ,  $R^0 = 5$ ,  $D^0 = 0$ ,  $L^0 = 5$ , and  $S^0 = N_{\text{ON}}^0 - I^0 - C^0 - R^0 - D^0 - L^0$ .
- In Quebec:  $I^0 = 1000$ ,  $C^0 = 1$ ,  $R^0 = 100$ ,  $D^0 = 1$ ,  $L^0 = 100$  and  $S^0 = N_{\text{QC}}^0 - I^0 - C^0 - R^0 - D^0 - L^0$ .

We take the following parameter values:

- In Ontario:  $\alpha = 0.03376598$ ,  $\beta = 0.75264002$ ,  $\gamma = 0.00030847$ ,  $\delta = 0.40388253$ ,  $\lambda = 0.07165674$ ,  $\kappa = 0.00790760$ ,  $\nu = 0.03453627$ .
- In Quebec:  $\alpha = 0.08742760$ ,  $\beta = 0.89581203$ ,  $\gamma = 0.02048859$ ,  $\delta = 0.30008983$ ,  $\lambda = 0.02118639$ ,  $\kappa = 0.00413191$ ,  $\nu = 0.04324828$ .

We consider 3 scenarios: total interprovincial lockdown i)  $\mathcal{S}_{\text{S,I,R}} = I$ , ii) no lockdown at all assuming that up to 0.1% of province population is susceptible to cross the border daily, and reduction by 90% of the reduction of the usual daily border crossing (that up to 0.01% cross the border daily), iii) and total lockdown.

This experiment shows that the provincial lockdown is an essential tool for reducing the spread of the disease and simultaneously reducing the overall number of deaths.

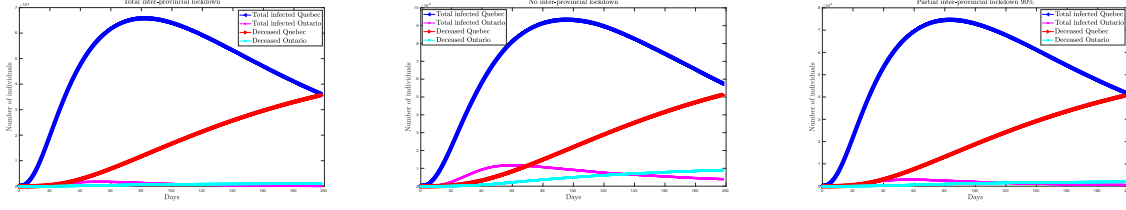


**Fig. 11 Inter-provincial lockdown.** (Left) Total inter-provincial lockdown (Middle) No inter-provincial lockdown. (Right) Partial inter-provincial lockdown (90%).

### 5.3 Including health condition

In order to make the modeling and prediction more accurate an important factor is population age and health condition. At this stage, we propose to add two categories per province: age/health conditions: “at risk” or “safe” regarding the death rate. Additional subgroups could easily added. We below detail the derivation for a given province. We denote by (S) (resp. (R)) the safe (resp. at risk) population index. For a total population  $N = N^{(S)} + N^{(R)}$ , with typically  $N^{(R)} \ll N^{(S)}$ . At risk population is typically old/non-healthy people. Rather than considering two sets of distinct parameters, we assume that some parameters are identical for both categories, such as,  $\beta = \beta^{(S)} = \beta^{(R)}$ ,  $\gamma = \gamma^{(S)} = \gamma^{(R)}$  and  $\delta = \delta^{(S)} = \delta^{(R)}$ . However  $\kappa$ ,  $\nu$  and  $\lambda$  are a priori distinct. We hence define a new set of parameters  $\mathbf{q} = (\alpha^{(R)}, \alpha^{(S)}, \beta, \gamma, \delta, \lambda^{(R)}, \kappa^{(R)}, \nu^{(R)}, \lambda^{(S)}, \kappa^{(S)}, \nu^{(S)})^T$ . We consider the systems

$$\frac{d\mathbf{Y}^{(R,S)}}{dt} = \mathcal{F}^{(R,S)}(\mathbf{Y}^{(R,S)}),$$

and the corresponding minimization.

$$E(\mathbf{q}) = \frac{1}{M} \sqrt{\sum_{n=1}^M \|\mathbf{Y}_k^{(R),n} - \bar{\mathbf{Y}}_k^{(R)}(t_n)\|_2^2 + \|\mathbf{Y}_k^{(S),n} - \bar{\mathbf{Y}}_k^{(S)}(t_n)\|_2^2}.$$

In the end, we simply get  $\mathbf{Y} = \mathbf{Y}^{(R)} + \mathbf{Y}^{(S)}$ .

**Lockdown policy.** The purpose of this last example, is to study the effect of partial confinement, more specifically the confinement of “at risk” population. In this example, we assume that 20% of the population is at risk, and has a death (resp. recovery) rate 100 (resp. 5) times higher than healthy population (young and no-comorbidity). We will compare total confinement of both populations, and lockdown rate 10 times less for healthy population. We assume that the other parameter are identical. The purpose of this example is to show that the confinement of at risk population allows to drastically reduce the overall number of deaths while limiting the social and economic impacts. In all the tests below, the initial data are identical given by

- Initial data:  $I^0 = 100$ ,  $C^0 = 10$ ,  $R^0 = 100$ ,  $D^0 = 10$ ,  $L^0 = 100$  and  $S^0 = N_{\text{Canada}}^0 - I^0 - C^0 - R^0 - D^0 - L^0$ ,
- For both population we take:  $\beta = 0.64498$ ,  $\gamma = 0.022128$ ,  $\delta = 0.26539$ ,  $\nu = 0.00007017$ .

and the total population number is fixed to  $3.7 \times 10^7$ . For partial confinement, see Fig. 12, we set the following data:

- “At risk” population.  $\alpha = 0.02141$ ,  $\lambda = 0.253665$ ,  $\kappa = 0.0094936$ .
- “Healthy” population.  $\alpha = 0.002141$ ,  $\lambda = 0.050733$ ,  $\kappa = 0.00009493$ .

For no confinement, see Fig. 13, , we have the following data:

- “At risk” population.  $\alpha = 0.002141$ ,  $\lambda = 0.253665$ ,  $\kappa = 0.0094936$ .
- “Healthy” population.  $\alpha = 0.002142$ ,  $\lambda = 0.050733$ ,  $\kappa = 0.00009493$ .

For total confinement, see Fig. 14, we have the following data:

- “At risk” population.  $\alpha = 0.02141$ ,  $\lambda = 0.253665$ ,  $\lambda = 0.050733$ ,  $\kappa = 0.0094936$ .

- “Healthy” population.  $\alpha = 0.02141$ ,  $\lambda = 0.050733$ ,  $\kappa = 0.00009493$ .

The experiments show the effect of confinements on the death numbers. Obviously, a total confinement allows for a very reduced number of deaths, partial confinement among the “at risk” population is essential for having a limited number of deaths. When the healthy population (which still contains some people which where not a priori at risk may still decease from the COVID-19) is not confined the number of deceases is still large but the overall number of deaths is 10 times lower than without confinement. It is then important to determine the reasonable objective from the sanitary and economic points of view, which is the purpose of the following subsection.

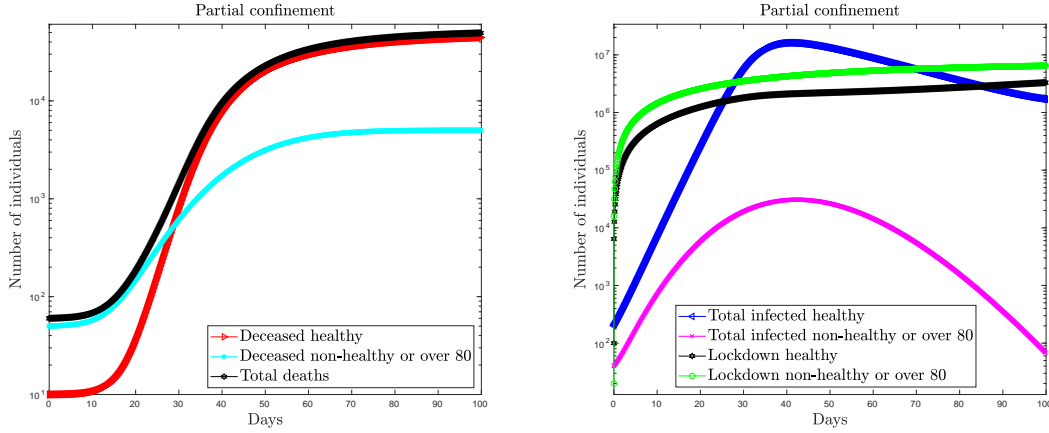


**Fig. 12 Lockdown policy.** Partial lockdown.

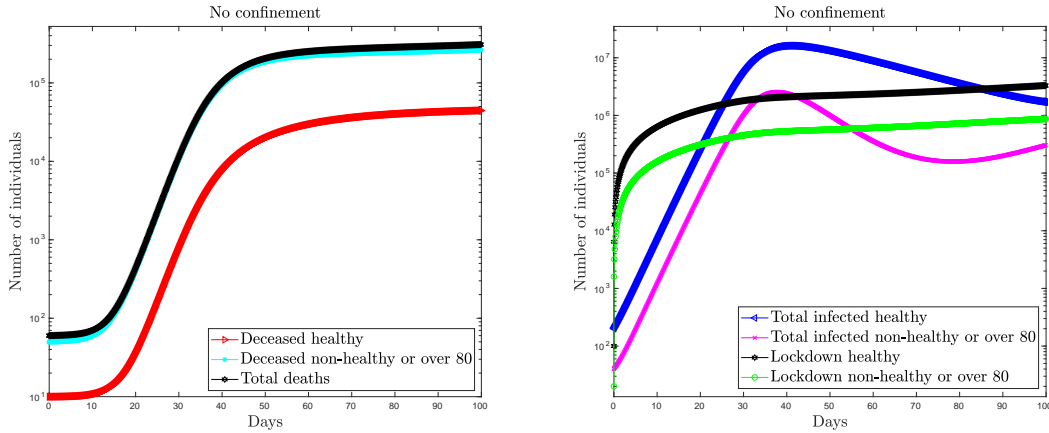


**Fig. 13 Lockdown policy.** No lockdown.

#### 5.4 Optimization of lockdown policy

In order to balance the sanitary lockdown and economic impact of the virus using the parameter  $\alpha^{(R,S)}$ , we propose to combine the model with an optimization algorithm. The objective is hence to minimize the disease-related deaths while maintaining a limited negative impact in the socio-economic impact (the larger  $\alpha^{(R,S)}$ , the larger the negative impact and the smaller the disease spread). We will also assume that the socio-economic impact of the society is  $K \in \mathbb{N}^*$  times higher for the S, then R population. This

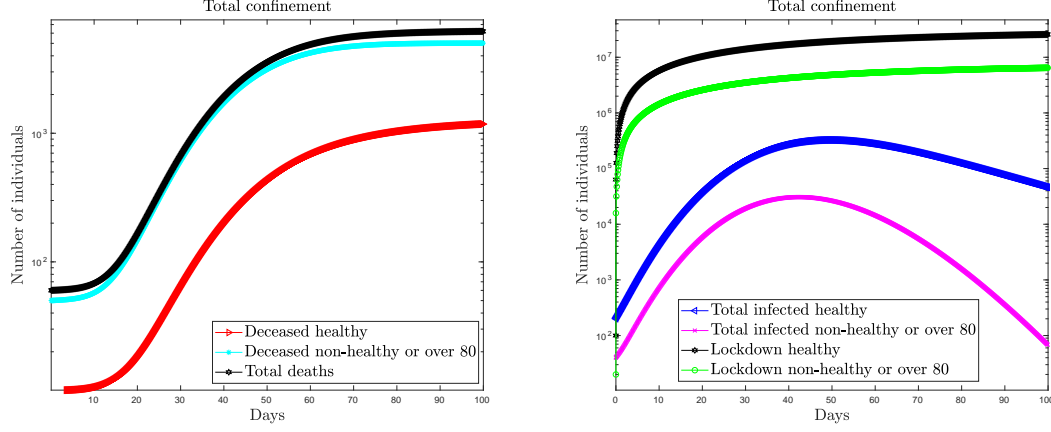


**Fig. 14 Lockdown policy.** Total lockdown.

is can be justified (at least economically) by the fact that healthy population is more “active”. Consider here one province, and the following systems

$$\frac{d\mathbf{Y}^{(R,S)}}{dt} = \mathcal{F}^{(R,S)}[\alpha^{(R,S)}](\mathbf{Y}^{(R,S)}),$$

where  $\alpha^{(R,S)}$  has to be optimized, based on the minimization of the following objective function as in [22]

$$\begin{aligned} \mathcal{J}[\alpha^{(R)}, \alpha^{(S)}] = & R^{(R)}(T) + R^{(S)}(T) + \mathcal{C} \left( \frac{1 - R_0(S^{(S)}(T) + S^{(S)}(T))}{1 - R_0 S_f} \right) \\ & + \int_0^T \mathcal{P}^R \mathcal{C}(\alpha^R) + \mathcal{P}^S \mathcal{C}(\alpha^S) dt, \end{aligned}$$

where  $\alpha = (\alpha^{(R)}, \alpha^{(S)})$ ,  $S_f = 0.95N/R_0$  and  $\mathcal{C} : x \mapsto x^2$ . The parameter  $\mathcal{P}^{(R,S)}$  is a control parameter which allows for considering different scenarios. We take  $\mathbf{Y}^{(R,S)}(0) = \mathbf{Y}_0^{(R,S)}$  with (R,S)-Systems read

$$\begin{cases} \dot{S}^{(R,S)} = -\beta \frac{S^{(R,S)} I^{(R,S)}}{N^{(R,S)}} - \alpha^{(R,S)}(t) S^{(R,S)} + \gamma R^{(R,S)} + \nu^{(R,S)} L^{(R,S)} \\ \dot{I}^{(R,S)} = \beta \frac{S^{(R,S)} I^{(R,S)}}{N^{(R,S)}} - \delta^{(R,S)} I^{(R,S)} \\ \dot{Q}^{(R,S)} = \delta I^{(R,S)} - \lambda^{(R,S)} Q^{(R,S)} - \kappa Q^{(R,S)} \\ \dot{R}^{(R,S)} = \lambda^{(R,S)} Q^{(R,S)} - \gamma R^{(R,S)} \\ \dot{D}^{(R,S)} = \kappa Q^{(R,S)} \\ \dot{L}^{(R,S)} = \alpha^{(R,S)}(t) S^{(R,S)} - \nu^{(R,S)} L^{(R,S)} \end{cases}$$

We apply a genetic algorithm in order to solve this optimization problem. We describ the optimization algorithm which is used in our simulations. We define the parameters describing the lockdown parameters  $\alpha^{(R,S)}$ .

- The parameters  $\alpha \in [\alpha_{\min}^{(R)}, \alpha_{\max}^{(R)}] \times [\alpha_{\min}^{(S)}, \alpha_{\max}^{(S)}]$ .
- We the set of parameters  $\alpha$ , we denote the parameter-dependent model by  $\partial_t \mathbf{Y}^{(R,S)} = \mathcal{F}[\alpha^{(R,S)}](\mathbf{Y}^{(R,S)})$ .

Let us detail the principle of the approach for minimizing  $\mathcal{J}$ . We iteratively compute the parameters  $\alpha$  in order to optimize

$$\min_{\alpha \in [\alpha_{\min}^{(R)}, \alpha_{\max}^{(R)}] \times [\alpha_{\min}^{(S)}, \alpha_{\max}^{(S)}]} \mathcal{J}[\alpha].$$

We then plan to construct a sequence  $\{\alpha_k\}_k$ , the simple following algorithm.



---

**Algorithm 2** Optimization algorithm.

---

**Result:**  $\min_{\alpha \in [\alpha_{\min}^{(R)}, \alpha_{\max}^{(R)}] \times [\alpha_{\min}^{(S)}, \alpha_{\max}^{(S)}]} \mathcal{J}[\alpha]$   
**Initialization:**  $\alpha_0 \in [\alpha_{\min}^{(R)}, \alpha_{\max}^{(R)}] \times [\alpha_{\min}^{(S)}, \alpha_{\max}^{(S)}]$   
**while** *Convergence criterion not satisfied* **do**  
    1. Solve  $\partial_t \mathbf{Y}^{(R,S)} = \mathcal{F}[\alpha_k^{(R,S)}] \mathbf{Y}^{(R,S)}$   
    2. Compute  $\mathcal{J}[\alpha_k]$   
    3. Update stochastically  $\alpha_{k+1} = \alpha_k + \delta \alpha_{k+1}$   
**end**

---

The following experiments,  $\alpha_{k+1} = (\alpha_{k+1}^{(R)}, \alpha_{k+1}^{(S)})$  we will be performed using function `ga` from `matlab` which implements a genetic algorithm, and possesses large number of options. Starting from an initial population is randomly chosen  $\alpha_0 \in [\alpha_{\min}^{(R)}, \alpha_{\max}^{(R)}] \times [\alpha_{\min}^{(S)}, \alpha_{\max}^{(S)}]$ , we proceed as follows until convergence:

- New population is updated and corresponding raw fitness scores are computed.
- Parents are selected using the expectation values.
- Children are produced *by making random changes to a single parent-mutation-or by combining the vector entries of a pair of parents-crossover*.
- Replace population.

Genetic algorithms allow for considering many more variables to be optimized. More complex optimization would then easily be implemented.

**Optimization of lockdown policy.** Let us consider a simple example. We propose an optimization of the lockdown parameter over 100 days, assuming 2 groups of individuals (at risk and healthy). We take the same data as the ones used in the **Lockdown policy** experiment, except for  $\alpha^{(R)}, \alpha^{(S)}$  which are searched in  $[2.141 \times 10^{-3}, 4.282 \times 10^{-2}] \times [2.141 \times 10^{-3}, 4.282 \times 10^{-2}]$ . In practice, we have chosen  $\mathcal{P}^{(R)} = 10^6$ ,  $\mathcal{P}^{(S)} = 10\mathcal{P}^{(R)}$  modeling that the lockdown of healthy (usually more economically active) population has more negative economic impact than at risk population (sick, older people, etc) often less active. As [22] we choose  $S_f = 0.95R_0/N$ . Optimization algorithm provides the following lockdown rate:  $\alpha^{(S)} = 4.155 \times 10^{-3}$  and  $\alpha^{(R)} = 1.814 \times 10^{-2}$ , which corresponds to a higher confinement among the “at-risk” population compared to the “healthy” one. The test shows a possible balance between sanitary and economic effects.

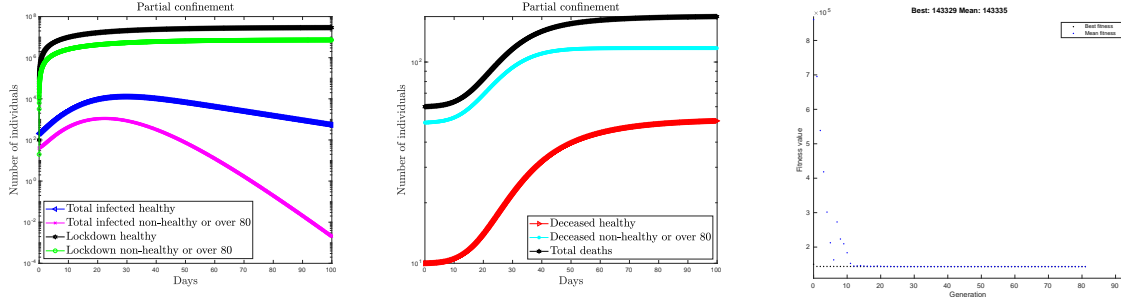


**Fig. 15 Optimization of lockdown policy.** (Left) Total variation of population in each province (Middle) Deceases per category. (Right) Objective functions.

## 6 Conclusion

In this article, an extended SIRS model including a lockdown component was derived in order to investigate the first wave of the COVID-19 pandemic in Canada and three of its provinces, Ontario, Québec and British Columbia. The model parameters were assumed constant, which was appropriate for the exponential growth phase of the coronavirus outbreak. However in a future work, time-dependent model parameters will be considered to perform more accurate studies, beyond the outbreak.

The values of the model parameters were computed thanks to the accessible data; this has allowed us to obtain overall, a good agreement between the calculated results and the available data. The results show that a large part of the population was insusceptible, which was indeed a success of lockdown policy. Several possible improvements were finally also proposed allowing for future accurate studies of different lockdown scenarios.

**Acknowledgements.** The authors would like to thank Natural Sciences and Engineering Research Council of Canada (NSERC) and Mathematics of Information Technology and Complex Systems (MITACS) for their financial support.

## References

1. <https://health-infobase.canada.ca/covid-19/>.
2. <https://resources-covid19canada.hub.arcgis.com/datasets/case-accumulation/data>.
3. <https://www.canada.ca/en/public-health/services/diseases/2019-novel-coronavirus-infection.html?topic=tilelink>.
4. S. A. Al-Sheikh. Modeling and analysis of an seir epidemic model with a limited resource for treatment. *Global Journal of Science Frontier Research Mathematics and Decision Sciences*, 12(14):56–66, 2012.
5. I. Berry, J.-P. R. Soucy, A. Tuite, and D. Fisman. Open access epidemiologic data and an interactive dashboard to monitor the covid-19 outbreak in canada. *CMAJ*, 192(15):E420–E420, 2020.
6. A. Bouchnita and A. Jebrane. A hybrid multi-scale model of covid-19 transmission dynamics to assess the potential of non-pharmaceutical interventions. *Chaos, Solitons & Fractals*, page 109941, 2020.
7. S. L. Chang, N. Harding, C. Zachreson, O. M. Cliff, and M. Prokopenko. Modelling transmission and control of the covid-19 pandemic in australia. *arXiv preprint arXiv:2003.10218*, 2020.
8. R. Dandekar and G. Barbastathis. Quantifying the effect of quarantine control in covid-19 infectious spread using machine learning. *medRxiv*, 2020.
9. M. De la Sen, A. Ibeas, S. Alonso-Quesada, and R. Nistal. On a new epidemic model with asymptomatic and dead-infective subpopulations with feedback controls useful for ebola disease. *Discrete dynamics in Nature and society*, 2017, 2017.
10. O. Diekmann, J. Heesterbeek, and J. A. Metz. On the definition and computation of the basic reproduction ratio  $R_0$  in models for infectious diseases in heterogeneous populations. *J. Math. Biol.*, 28(4):365–382, 1990.
11. R. Djidjou-Demasse, Y. Michalakisa, M. Choisy, M. Sofonea, and S. Alizon. Optimal covid-19 epidemic control until vaccine deployment. *medrxiv* (2020). DOI, 10(2020.04):02–20049189, 2020.
12. R. Engbert, M. M. Rabe, R. Kliegl, and S. Reich. Sequential data assimilation of the stochastic seir epidemic model for regional covid-19 dynamics. *medRxiv*, 2020.
13. A. Eshragh, S. Alizamir, P. Howley, and E. Stojanovski. Modeling the dynamics of the covid-19 population in australia: A probabilistic analysis. *arXiv preprint arXiv:2005.12455*, 2020.
14. N. Ferguson, D. Laydon, G. Nedjati-Gilani, N. Imai, K. Ainslie, M. Baguelin, S. Bhatia, A. Boonyasiri, Z. Cucunubá, G. Cuomo-Dannenburg, et al. Report 9: Impact of non-pharmaceutical interventions (npis) to reduce covid19 mortality and healthcare demand. *Imperial College London*, 10:77482, 2020.
15. D. Fisher and D. Heymann. Q&a: The novel coronavirus outbreak causing covid-19. *BMC medicine*, 18(1):1–3, 2020.
16. S. Flaxman, S. Mishra, A. Gandy, H. Unwin, H. Coupland, T. Mellan, H. Zhu, T. Berah, J. Eaton, P. P. Guzman, et al. Report 13: Estimating the number of infections and the impact of non-pharmaceutical interventions on covid-19 in 11 european countries. 2020.
17. R. Ghanam, E. L. Boone, and A.-S. G. Abdel-Salam. Seird model for qatar covid-19 outbreak: A case study. *arXiv preprint arXiv:2005.12777*, 2020.
18. R. Ghanam, E. L. Boone, and A.-S. G. Abdel-Salam. Seird model for qatar covid-19 outbreak: A case study. *arXiv preprint arXiv:2005.12777*, 2020.
19. J. K. Hale. Ordinary differential equations, 1969. 1969.
20. P. Hartman. Ordinary differential equations, ser. *Classics in Applied Mathematics*, 2nd ed. Philadelphia, PA: Society for Industrial and Applied Mathematics, 2002.
21. J. Jia, J. Ding, S. Liu, G. Liao, J. Li, B. Duan, G. Wang, and R. Zhang. Modeling the control of covid-19: Impact of policy interventions and meteorological factors. *arXiv preprint arXiv:2003.02985*, 2020.
22. M. Kantner and T. Koprucki. Beyond just "flattening the curve": Optimal control of epidemics with purely non-pharmaceutical interventions. 2020.
23. S. Khailaie, T. Mitra, A. Bandyopadhyay, M. Schips, P. Mascheroni, P. Vanella, B. Lange, S. Binder, and M. Meyer-Hermann. Estimate of the development of the epidemic reproduction number  $R_t$  from coronavirus sars-cov-2 case data and implications for political measures based on prognostics. *medRxiv*, 2020.
24. S. Kim, J. H. Byun, and I. H. Jung. Global stability of an seir epidemic model where empirical distribution of incubation period is approximated by coxian distribution. *Advances in Difference Equations*, 2019(1):469, 2019.
25. A. J. Kucharski, T. W. Russell, C. Diamond, Y. Liu, J. Edmunds, S. Funk, R. M. Eggo, F. Sun, M. Jit, J. D. Munday, et al. Early dynamics of transmission and control of covid-19: a mathematical modelling study. *The lancet infectious diseases*, 2020.
26. J. P. LaSalle. The stability of dynamical systems, cbms-nsf reg. In *Conf. Ser. Appl. Math. SIAM*, Philadelphia, 1976.
27. V. M. Marquioni and M. A. M. de Aguiar. Quantifying the effects of quarantine using an ibm seir model on scalefree networks. *arXiv preprint arXiv:2005.14127*, 2020.
28. K. McIntosh, M. S. Hirsch, and A. Bloom. Coronavirus disease 2019 (covid-19). *UpToDate Hirsch MS Bloom*, 5, 2020.

29. K. Y. Ng and M. M. Gui. Covid-19: Development of a robust mathematical model and simulation package with consideration for ageing population and time delay for control action and resusceptibility. *Physica D: Nonlinear Phenomena*, page 132599, 2020.
30. World Health Organization. Rolling updates on coronavirus disease (covid-19).[cited 2020 april 14] available at: <https://www.who.int/emergencies/diseases/novel-coronavirus-2019/events-as-they-happen>. 2020.
31. A. Rezabakhsh, A. Ala, and S. H. Khodaie. Novel coronavirus (covid-19): a new emerging pandemic threat. *Journal of Research in Clinical Medicine*, 8(1):5–5, 2020.
32. M. A. Safi and S. M. Garba. Global stability analysis of seir model with holling type ii incidence function. *Computational and mathematical methods in medicine*, 2012, 2012.
33. J. L. Sesterhenn. Adjoint-based data assimilation of an epidemiology model for the covid-19 pandemic in 2020. *arXiv preprint arXiv:2003.13071*, 2020.
34. H. L. Smith and P. Waltman. *The theory of the chemostat: dynamics of microbial competition*, volume 13. Cambridge university press, 1995.
35. M. Tahir, N. Anwar, S. I. A. Shah, and T. Khan. Modeling and stability analysis of epidemic expansion disease ebola virus with implications prevention in population. *Cogent Biology*, 5(1):1619219, 2019.
36. F. Wu, S. Zhao, B. Yu, Y.-M. Chen, W. Wang, Z.-G. Song, Y. Hu, Z.-W. Tao, J.-H. Tian, Y.-Y. Pei, et al. A new coronavirus associated with human respiratory disease in china. *Nature*, 579(7798):265–269, 2020.
37. C. W. Yi, S. C. Ching, and J. C. Yu. The outbreak of covid-19: An overview. 2020.
38. H. Zhang, L. Yingqi, and W. Xu. Global stability of an seis epidemic model with general saturation incidence. *ISRN Applied Mathematics*, 2013, 2013.
39. N. Zhu, D. Zhang, W. Wang, X. Li, B. Yang, J. Song, X. Zhao, B. Huang, W. Shi, R. Lu, et al. A novel coronavirus from patients with pneumonia in china, 2019. *New England Journal of Medicine*, 2020.